The study of heat transfer enhancement of solar air heater using airfoiled extended surface

By

Liew Minzhao

18145

Dissertation submitted in partial fulfilment of

as a Requirement for the

Bachelor of Engineering (Hons)

(Mechanical)

January 2017

Universiti Teknologi PETRONAS

Bandar Seri Iskandar

31750 Tronoh

Perak Darul Ridzuan

CERTIFICATION OF APPROVAL

The study of heat transfer enhancement of solar air heater using airfoiled extended surface

by

Liew Minzhao

18145

A project dissertation submitter to the

Mechanical Engineering Programme

Universiti Teknologi PETRONAS

In partial fulfilment of the requirement for the

BACHELOR OF ENGINEERING (Hons)

(MECHANICAL)

Approved by,

____

(Dr. Jundika Candra Kurnia)

UNIVERSITI TEKNOLOGI PETRONAS

BANDAR SERI ISKANDAR, PERAK

January 2017

CERTIFICATION OF ORIGINALITY

This is to certify that I am responsible for the work submitted in this project, that the original work is my own except as specified in the references and acknowledgements, and that the original work contained herein have not been undertake or done by unspecified sources or persons.

LIEW MINZHAO

ABSTRACT

Over the last decades, solar air heaters (SAHs) are widely use all around the world. It is recognized as one of the most popular solar energy utilization system which uses fundamental of heat transfer to collect and convert solar energy to heat energy for air, space, working fluid and more. Solar energy from the Sun is collected by this device through a surface which is called absorber plate through convection and radiation, the energy is then transferred to the working fluid or space by using convection and radiation. Although solar air heaters using nowadays are performing well and fine, there is still room for further improvement on its performance and efficiency.

Researches has been done on improving and enhancing the performance of solar air heater by different kinds of ways. The most popular approach is by adding fins with different kinds of shapes, such as circular, square, cylindrical etc. However, there's still no research made by far to study about the effect of having NACA Airfoil shaped fins into solar air heater. Therefore, the main objective of this study is to investigate the performance of solar air heater enhancement by adding NACA Airfoil shape fins.

The study will be conducted by utilizing computational fluid dynamics (CFD) approach and the model will be developed based on correlation of mass, momentum and energy. The performance of solar air heater with and without fin were compared based on the obtained numerical results. The model with small fins has a better thermal performance than default model, but at the same time experiencing more energy loss in terms of pressure drop due to increase in shear friction force. However, after comparing both performance together, model with fins shows higher overall thermal-hydraulic performance than datum.

In a nutshell, this study provides guidance for further research on the effect of addition NACA Airfoil shaped fins towards the performance of solar air heater.

ACKNOWLEDGEMENTS

Special appreciation goes to my supervisor, Dr.Jundika Candra Kurnia for all the guidance and teaching throughout the whole semester. Without having all the help, the progress of my project wouldn't be as smooth as it is for now. All the knowledge and information shared will not be wasted and will assist me in my future life.

Next, I will like to thank my internal examiner, Prof Dr Hussain H. Al-Kayiem for giving me all the suggestion and guidance throughout my presentation and submission. Due to his unselfishness teaching and sharing, I'm able to improve not only the project, but also myself in terms of life and studies. Furthermore, thank you for all the patience and understanding throughout the hard times that I'm been through during the semester.

Finally, I will like to show my appreciation and gratitude to the coordinates for FYP I and II, Dr. Turnad and Dr. Tamiru for assisting us students in finishing our final year project. Thank you for conducting all the classes and seminars to teach us proper way of preparing reports, technical papers and dissertation. Having all the guidance ease the process of preparation for the reports and also helps in improving the quality of our technical papers and dissertation, which helps us in improving our grades.

TABLE OF CONTENT

LIST OF FIGURES

LIST OF TABLES

CHAPTER 1: INTRODUCTION

1.1 Background Study

Solar air heating is the conversion of solar radiation to thermal heat, where the thermal heat is absorbed and transferred by working fluid or air, which is then delivered to living or working space. However, due to the transparent property of air, heat energy is not absorbed into it 100%. Therefore, solar air heaters are created and used to act as a tool which enhance and increase the efficiency of heat transfer to the air and deliver the air to the designated destination. From here, we can see that solar air heaters work along with operation basics and fundamental thermodynamic principles, which are:

As the society keep on improving and advancing in the technology aspect, people keep finding ways to improve the machines or instruments that they are currently using to save up more cost and time by improving the efficiency. This falls the same to solar air heater; numerous researches had been done about how to improve the efficiency and performance of solar air heaters. Some example of methods to improve solar air heaters are:

1. Adding dimple-shape artificial roughness along the duct of a solar air heater
2. Increase the pumping power for the solar air heater
3. Adding fins into the solar air heater to improve the heat transfer

After studying through lots of research papers, it is found that the most popular method of enhancing the performance of solar air heater is by adding extended surface (or fins), which improve performance by increasing heat transfer area and introducing turbulent flow. However, there is a critical problem caused by turbulent flow: outlet pressure drops to a certain level where energy lost is too high to be bare [1-8]. NACA Airfoil can be used to introduce turbulent flow and able to minimize pressure drop by placing it in a specific arrangement[9, 10].

1.2 Problem Statement

i. Researches had been done towards the effect of addition fins with different shapes: circular, cylindrical, square etc. However, there is still no research been done on the effect of NACA Airfoil shaped fins towards the performance of Solar Air Heater.
ii. Pressure drop has been the main problem for solar air heater with the application of additional fins and the overall performance of solar air heater depends on both thermal and hydraulic performance.

1.3 Objectives and Scope of Study

The objective of the proposed study

i. To investigate the performance of solar air heater enhancement by utilizing airfoil shape fins.
ii. To evaluate the key parameters (size, arrangement) affecting the performance of solar air heater.

The scopes of the proposed study are:

i. The study focus on numerical investigation
ii. NACA airfoil shape will be chosen as fin
iii. The working fluid is air which have temperature dependent properties
iv. Reynolds numbers (lowest value) to (highest value) will be investigated.

CHAPTER 2: LITERATURE REVIEW

2.1 Solar Air Heater

Yadav and Bhagoria stated that due to the rapid improvement and advancement of technology, twenty-first century has slowly steps into the perfect energy storm[11]. The changing of global energy phenomena are changing rapidly nowadays due to the increasing energy prices, reducing energy sources and security, and lastly the growing of environmental concerns[12]. Due to these issues, renewable energy has become a new trend towards to society. Solar air heaters (SAH) are widely used throughout the whole world for energy conservation and management, and it has been recognized as the foremost component of solar energy utilization system[11-17]. The main reasons why solar air heaters are so popular among the society are because of its simplicity in design, cheap in cost, availability of materials, economy of operation and maintenance etc[12-14]. Solar air heaters are used mainly to receive or absorb thermal radiation from the Sun, which act as source of energy, and convert it into thermal energy at the absorbing surface, then transfer all the energy to a specific space or working fluid. The common applications of solar air heaters are: space heating, curing or drying of concrete or clay building components and industrial products, drying of agricultural crops, timber seasoning etc[11-15, 17].

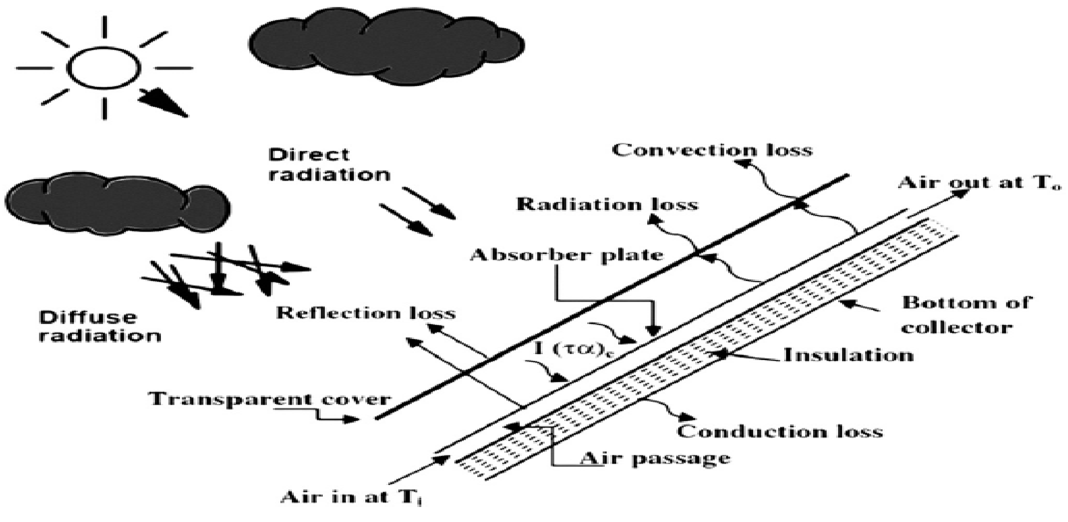

Figure 1: Solar Air Heater

Solar air heaters are mainly divided into two types: solar air heaters with non-porous or porous absorber plate. The main difference between this two types of air heaters is the flow of the air streams: for non-porous absorber plate solar air heater, the air flows only above or below the absorber tray, as for porous absorber plate solar air heater, the air can flow through the absorber tray. The main disadvantage for non-porous solar air heater is it required to capture all the incoming solar radiation over the projected area only through a thin layer over the surface of absorber tray[12].

For a conventional solar air heater, it generally consists of:

Table 1: Main parts of Solar Air Heater

Part	Description
Duct	1. To supply fresh air and exhaust hot or warm air by natural or forced convection 2. Air velocity – the main factor in affecting the efficiency
Glazing	1. A transparent glass that plays an important role in allowing incident solar radiation entering the devide and at the same time reducing or restricting losses of infrared energy through re-radiation. 2. The main reason of using a transparent glass is to minimize convection losses from the absorber plate to the environment through the restraint of stagnant fluid layerin between the absorber and glazing.
Blower	1. To control the fluid motion inside the solar air heater. 2. Fluid motion is very important in affecting the convection heat transfer. It is categorized into two basic flow: (i) Natural convection, (ii) Forced convection. 3. Natural convection – fluid motion generated by gravitaional fields. 4. Forced convection – fluid motion generated mechanically by using fan, pump, blower etc.

	5. Most of the solar air heater uses forced convection because it improves the heat transfer rate and provides an excellent flow rate of the hot air for space heating.
Absorber Tray	1. Main component for solar air heater, which is used to collect or absorb solar radiation from the source. 2. Momentously affect the overall thermal performance and cost of solar air heater. 3. Main aspect that affects the thermal performance will be the material and main properties of the absorber tray.
Insulation	1. Simplest way to reduce heat losses and to achieve high economy efficiency in energy usage. 2. Functions: (i)conserve energy, (ii)reduce heat loss, (iii)maintain operational efficiency of the system, (iv)helps in maintaining constant temperature

There are a few methods are used to improve the efficiency and performance of solar air heater. One of the method to improve the performance of solar air heater is to increase the fluid flow velocity or to introduce turbulent flow. According to Yunus and Ghajar[18], the author for the book “Heat and Mass Transfer”, turbulent flow is much more disordered and rapid compare to laminar flow, where the high velocity flow causes swirling regions in the fluid which is known as eddies. These swirling eddies transport mass, energy and momentum much faster than molecular diffusion, and thus enhancing mass, momentum and heat transfer. However, pressure level will drop accordingly with the increase of fluid velocity[18], which will be the main concern for this method as higher pressure drop means that higher energy are consumed. In order to make a economically viable solar air heater, thermal efficiency needs to be increase by improving heat transfer coefficient, which can be achieve by introducing fully turbulent flow while the same time maintaining the pressure drop in an appropriate rate[16].

In conclusion, pressure drop has been the biggest problem faced by solar air heater with additional fins and needed to be solved in order to improve the overall efficiency.

2.2 NACA Airfoils

Albert, Dornhoff and Louis mentioned that methodology of NACA airfoil has been started since early of 1930s when a NACA report with the title of "The Characteristic of 78 Related Airfoil Sections from Tests in the variable Density Wind Tunnel". There are different series of NACA airfoils, however the author of the report emphasizes on two primary variables which give the most impact on the shapes of the airfoils, which is the slope of the airfoil mean chamber line and also the thickness distribution above and below the line. The differences between the different series NACA airfoils are shown below:

Table 2: List for Types of NACA Airfoil

Family	Advantage	Disadvantage
4-Digit	1. Good stall characteristics 2. Small center of pressure movement across large speed range. 3. Roughness has little effect	1. Low maximum lift coefficient 2. Relatively high drag 3. High pitching moment
5-Digit	1. Higher maximum lift coefficient 2. Low pitching moment 3. Roughness has little effect	1. Poor stall behavior 2. Relatively high drag
6-Series	1. High maximum lift coefficient 2. Very low drag over a small range of operating conditions 3. Optimized for high speed	1. High drag outside of the optimum range of operating conditions 2. High pitching moment 3. Poor stall behavior 4. Very susceptible to roughness

7-Series	1. Very low drag over a small range of operating conditions 2. Low pitching moment	1. Reduced maximum lift coefficient 2. High drag outside of the optimum range of operating conditions 3. Poor stall behavior 4. Very susceptible to roughness
16-Series	1. Avoids low pressure peaks 2. Low drag at high speed	1. Relatively low lift

By using the fundamental of NACA airfoils, it can be used as one of the method to enhance the performance of solar air heater, which is by adding NACA airfoil shaped fins. According to journal paper from the author Gim and Lee, by placing NACA airfoils at a certain angle in the middle of a fluid flow will cause the flow behind it to be turbulence. Furthermore, studies has shown that different arrangements of fins in the solar air heater have different results[9, 19]. For example, solar air heater with staggered arrangement of fins results in lower pressure drop compare to the one using unstaggered arrangement. While the one with vertical and horizontal arrangement has a higher heat transfer.

In a nutshell, NACA Airfoil has the ability to decrease or reduce pressure drop by having the right arrangement and pattern. This knowledge is believed to be applicable for solar air heater as well.

CHAPTER 3: METHODOLOGY

3.1 Mathematical Model

3.1.1 Governing Equation

In order to measure and analyse the performance of the solar air heater, there are a few calculations that will be used as guideline for this project. According to Yadav and.Bhagoria[2], performance of any system can be represented by the degree of utilization of input to the system. There's a few types of performances that can be measured in order to determine the efficiency of solar air heater, such as: (i) Thermal performance, (ii) Hydraulic performance and (iii) Thermo-hydraulic performance.

i. Thermal performance

Thermal performance is used to measure and analyse the heat transfer process within the solar air heater[11]. It can be calculated by using the Hottle Whillier-Bliss equation which is reported by Duffie and Beckman:

$$Q_u = A_c.F_R.[I(\tau\alpha)_e - U_L(T_i - T_a)] \quad (1)$$

Or

$$q_u = \frac{Q_U}{A_c} = F_R.[I(\tau\alpha)_e - U_L(T_i - T_a)] \quad (2)$$

Where: Q_u = useful heat gain (W)

A_c = surface area of absorber plate (m^2)

I = turbulence intensity (W/m^2)

$(\tau\alpha)_e$= effective transmittance-absorptance product

U_L = overall heat loss coefficient (W/m^2K)

T_i = fluid inlet temperature (K)

T_a = ambient temperature (K)

q_u = useful heat flux

Next, we can measure the rate of effective energy gain by the flowing fluid in the duct of a solar air heater by using this equation:

$$Q_U = \dot{m} \, . C_p \, (T_o - T_i) = h. A_c (T_{pm} - T_{am}) \quad (3)$$

Where: $\dot{m}$ = mass flow rate

C_p = specific heat of air (J/kg.K)

T_o = fluid outlet temperature (K)

T_i = fluid inlet temperature (K)

h = heat transfer coefficient (W/m^2K)

A_c = surface area of absorber plate (m^2)

T_{pm} = mean plate temperature (K)

T_{am} = mean air temperature (K)

ii. Hydraulic performance

Hydraulic performance concerns about the pressure drop of the solar air heater in the duct, where the pressure drop indicates that more energy are consume from the blower in order to provide the same propelling force of the air through the duct[11]. For fully turbulence flow through duct with Reynolds number less than 50000, pressure drop can be calculated by using this equation:

$$\frac{\Delta P}{l} = \frac{f_d \rho v^2}{2D} \quad (4)$$

Where: ΔP = pressure drop (Pa)

f_d = Darcy-Weisbach friction factor

ρ = density of air (kg/m^3)

l = length of duct (m)

v = velocity of air in the duct (m/s)

D = equivalent or hydraulic diameter of duct (m)

By substituting Darcy-Weisbach friction factor with fanning friction factor ($f_d = 4f$):

$$\Delta P = \frac{2 f \rho l v^2}{D} \quad (5)$$

iii. Thermo-hydraulic performance

In order to be able to judge the performance of a newly designed solar air heater, both thermal and hydraulic performance must be taken into account[11]. The most desirable design of solar air heater must have a maximum heat energy transfer with minimum consumption of blower energy. Therefore, the term thermo-hydraulic performance has been created to connect both thermal and hydraulic performance together, which will consider both thermal and hydraulic characteristcs simultaneously. The index which represents thermo-hydraulic performance of solar air heater is:

$$Thermo - hydraulic\,performance = \frac{Nu/Nu_s}{(\frac{f}{f_s})^{1/3}} \quad (6)$$

Where: Nu = Nusselt number

Nu_s = smooth Nusselt number

f = friction factor

f_s = smooth friction factor

Besides calculation, Computation Fluid Dynamics Method will be used as the main method of analyzing the performance and results of the solar air heater. By using CFD, graphs and pictures about the rate of heat transfer and pressure level can be generated, which will allow and ease our analysis and validation process. Furthermore, inside CFD program, all the formula related to heat transfer and fluid dynamics are included, therefore the program will generate the results and figures that we needed automatically. This project will mainly be focusing on numerical study on the performance of solar air heater as there are too many factors that need to be included in the simulation to get the exact results. However, the result obtain from this project will be accurate enough to be used for future development of solar air heater.

3.1.2 Constitutive relation

Reynolds number for the working fluid in solar air heater is calculated by using the formula:

$$Re = \frac{\rho v D}{\mu} \tag{7}$$

Where:

1. Re = Reynolds number
2. ρ = Density of air
3. v = Inlet velocity of air, m/s
4. D = hydraulic diameter, m
5. μ = dynamic viscosity of air, kg/(m·s).

Convective heat transfer coefficient value for each location within the solar air heater will be calculated by using the formula below:

$$h = \frac{Q}{T_s - T_m} \tag{8}$$

where: Q = Average heat flux = 454.54$\frac{W}{m^2}$

T_s = Surface temperature

T_m = Mean temperature

Average value of convective heat transfer coefficient will be calculated and used to find Nusselt number with the formula:

$$Nu = \frac{h \times D_h}{k} \tag{9}$$

Where Nu = Nusselt number

h = convection heat transfer coefficient

D_h = Hydraulic diameter

k = conductive heat transfer coefficient

3.1.3 Boundary Condition

The boundary condition for the simulation will be:

1. Fluid flow will be air (density =1.225$\frac{kg}{m^3}$, specific heat capacity =1006.43$\frac{J}{kg.K}$, Prandlt number = 0.744, thermal conductivity k = 0.0242$\frac{W}{m.K}$).
2. Turbulence condition is assumed: the range of Reynolds number used: 10000 to 15000
3. Inlet velocity is calculated by changing the arrangement of the formula used to calculate Reynolds number:

$$v = \frac{Re\mu}{\rho D} \tag{10}$$

4. Constant heat flux applied top side of the walls (Heat flux=1000$\frac{W}{m^2}$).
5. Outlet pressure remains as atmospheric pressure($\frac{dP}{dt} = 0$).

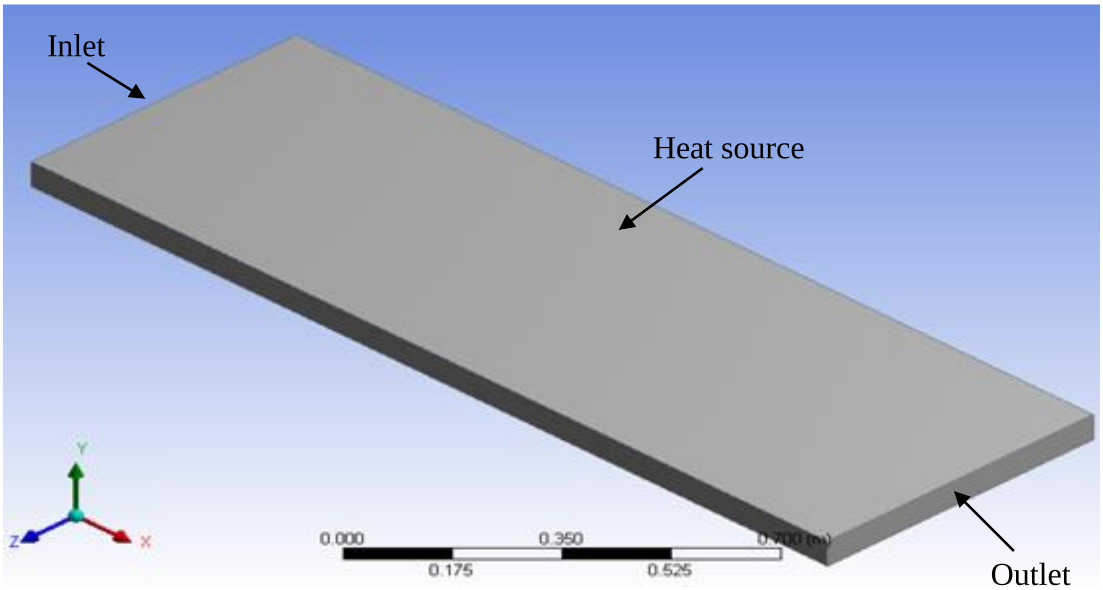

Figure 2: Major component for the model

3.2 Validation for best Turbulence model

In ANSYS, there are at least 4 types of turbulence model can be chosen. Therefore, validation must be done to find out which model is the most suitable one that provide the most accurate result.

There's a total of 5 models that had been chosen to run the validation: K-epsillon RNG, K-epsillon Standard, K-omega Standard, K-omega SST and K-omega BSL. For each model, simulation is ran with the same range of Reynolds Number: 15000 to 30000, and the Nusselt number is calculated and compared with the value calculated from Dittus-Boelter Equation.

$$Nu = 0.023Re^{0.8}Pr^{0.4} \tag{11}$$

The graph produced by this equation will be used as a datum, and the model that produces the graph nearest to this graph will be the most accurate model among all of them.

Below shows a table and graph related to the results:

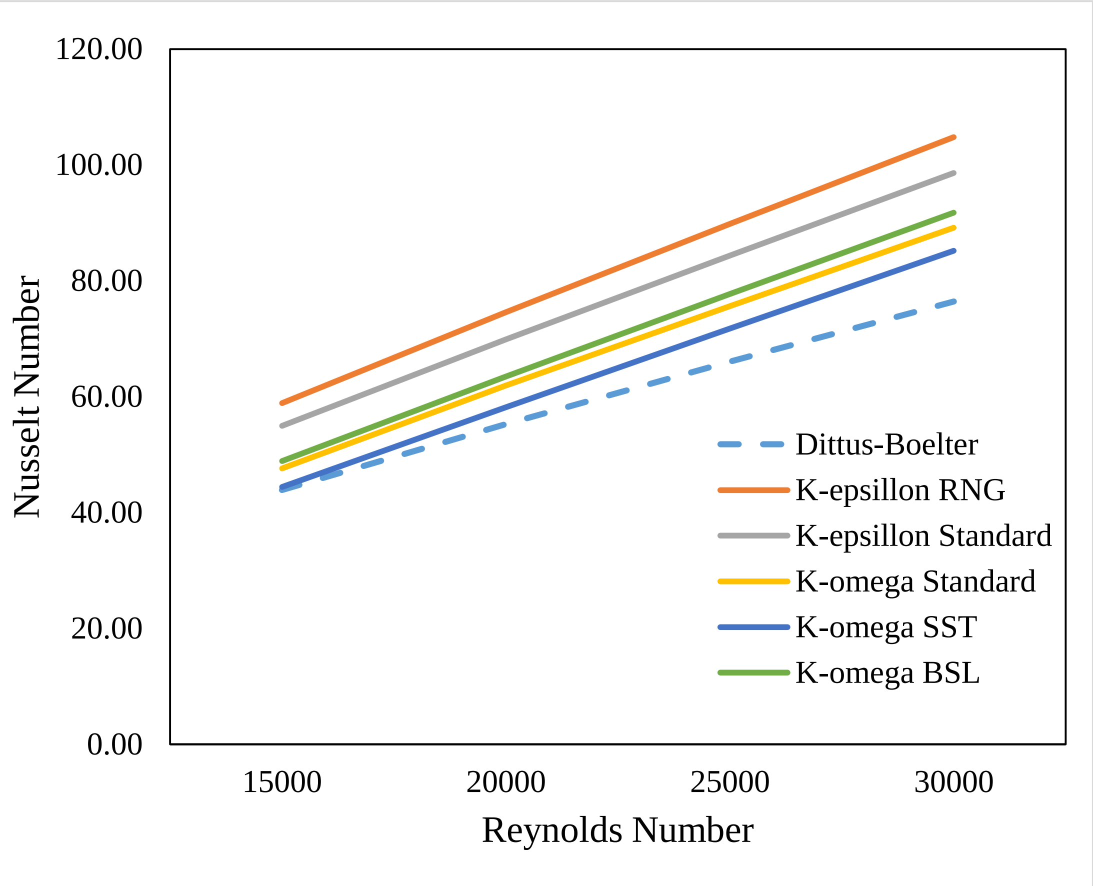

Figure 3: Graph Nusselt number vs Reynolds number (Validation Process)

Table 3: Results from simulation (Model Validation)

Reynolds Number	Nusselt Number					
	Dittus-Boelter	K-epsillon RNG	K-epsillon Standard	K-omega Standard	K-omega SST	K-omega BSL
15000	43.89	58.88	54.95	47.60	44.42	48.89
20000	55.25	74.56	69.86	61.94	58.14	63.47
25000	66.05	89.82	84.37	75.60	71.73	77.75
30000	76.42	104.78	98.59	89.18	85.18	91.77

After comparing the results from each model, K-omega SST model produces results closes with the results obtained from Dittus-Boelter equation. Therefore, K-omega SST model is chosen to be used for the simulation.

3.3 Meshing Independent Analysis

Meshing Independent Analysis is important to identify and find out what will be the suitable meshing size to use for the simulation. Too large meshing size may cause weak or inaccurate result, while too small meshing size will not be favorable even if the result will be accurate but still the simulation will take too long and more time will be wasted in between. There will be a point where the meshing size will not come to be a factor in affecting the result obtained, and this will be the most ideal meshing size for the simulation, which we can use to obtain accurate result without having to waste any of our precious time.

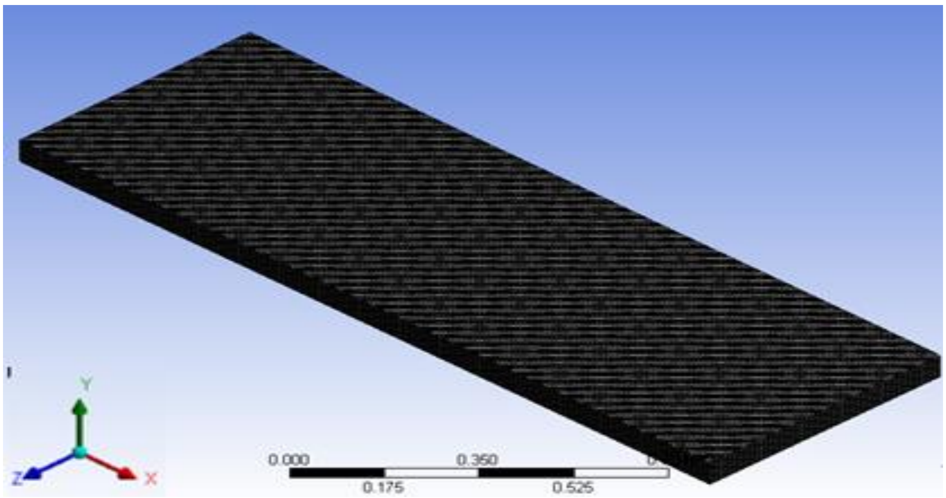

Figure 4: Model used for Meshing Independent Analysis and Validation process

After having to select the correct model, simulations are ran using the correct model, by having the same value of Reynolds number and different size of meshing, Nusselt number is calculated and plotted into graph to observe the trend. Below shows a table and graph produced from the result obtained from simulation:

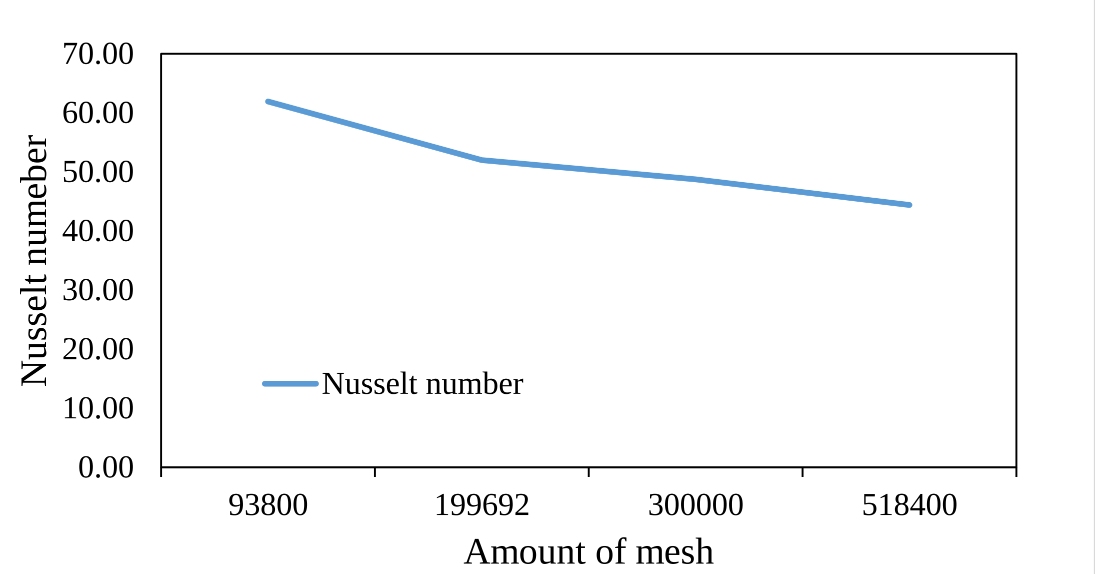

Figure 5: Nusselt number vs Amount of mesh (Meshing Independent Analysis)

Table 4: Results obtained from simulation (Meshing Independent Analysis)

Amount of mesh	Re	Q (W)	Average temperature of perimeter (K)	Outlet temperature (K)	h (W/(m^{2}K))	Hydraulic diameter (m)	k (W/(m^{2}K))	Nu
93800	15000	454.55	346.17	313.08	13.74	0.1091	0.0242	61.93
199692	15000	454.55	352.76	313.34	11.53	0.1091	0.0242	51.98
300000	15000	454.55	355.45	313.43	10.82	0.1091	0.0242	48.77
511900	15000	454.55	359.69	313.54	9.85	0.1091	0.0242	44.40

From the results obtained, we can see that the changes of Nusselt number is still quite large. However, the Nusselt number value produced from 518400 mesh is already close to the theoretical value calculated from Dittus-Boelter equation. Due to the constriction of the using program (ANSYS Student version 17.1 only allows 512000 as the maximum amount of meshing), the meshing of 511900 will be chosen for our simulation.

3.4 Development of Models

There are a total of 7 models of solar air heater will be compared against each other to find out which design will have the highest efficiency: high rate of heat transfer with low and acceptable pressure drop. The first model will be a normal solar air heater without any fins inside. This model act the datum among all the models of this project, which is used as a bottom line limit indicator whereby the result delivered by this model is the minimum requirement for a solar air heater. This model is developed straightly inside the ANSYS program due to the simplicity of shape and design of the model.

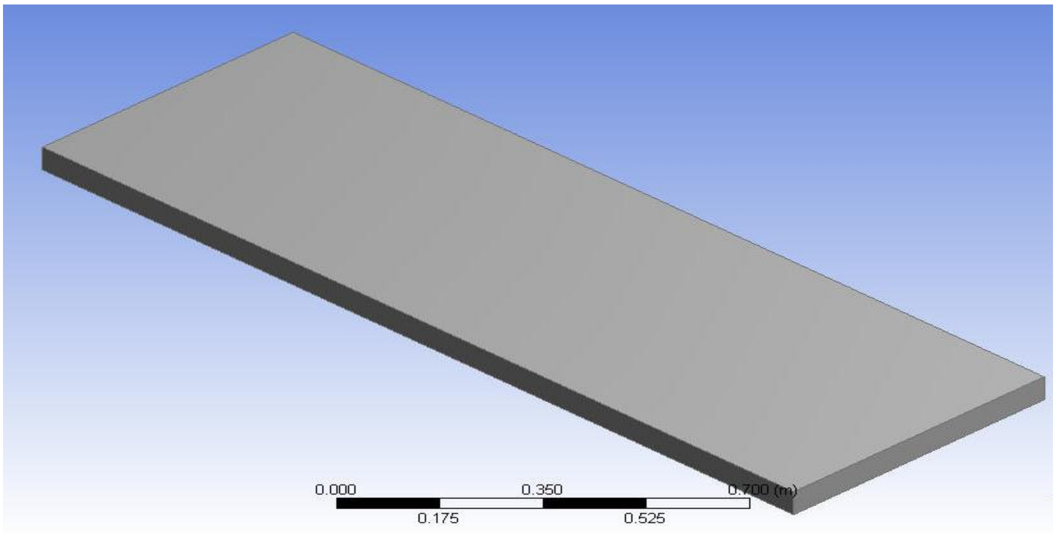

Figure 6: Typical Solar Air Heater without any fins (Datum)

The next 6 solar air heaters are models with NACA airfoil shaped fins inside. The difference between these models are the arrangement of the fins: horizontal arrangement and staggered arrangement. Both designs will be the main design for my final year project: after so much literature reviews were done towards NACA airfoil and its effect to heat transfer efficiency, it is expected to help in increasing the efficiency of solar air heater. NACA Airfoil 0012 is chosen to use as our fin's shape for our project, and the coordinates are retrieved from the internet. There will be 3 types of models: 5cm, 10cm and 20cm fin size for each staggered and horizontal arrangement. All models are developed through ANSYS Fluent in order to avoid any unexpected failure or imperfection occur during meshing and simulation process. The location of the fins on the models are carefully placed to ensure that the gap and distance between the fins are not too close.

The size of every models is set to be the same to ensure more accurate and consistent results to be obtained, so that comparison can be done correctly and accurately. The size of the models is: 1.2m long, 0.6m wide and 0.06m thick. Below show pictures for each model with fins:

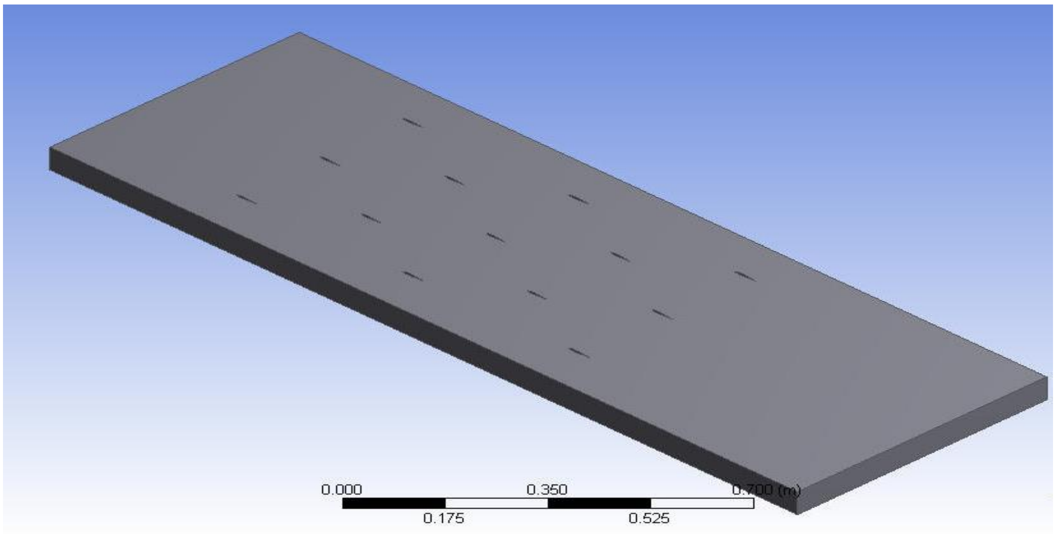

Figure 7: Model with Staggered NACA Airfoil Fins (5cm)

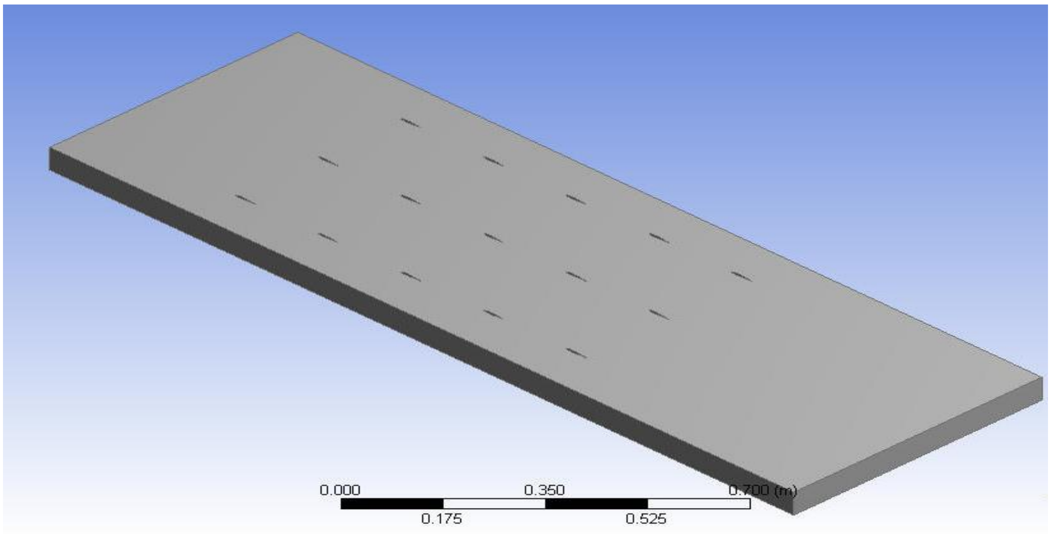

Figure 8: Model with Horizontal NACA Airfoil Fins (5cm)

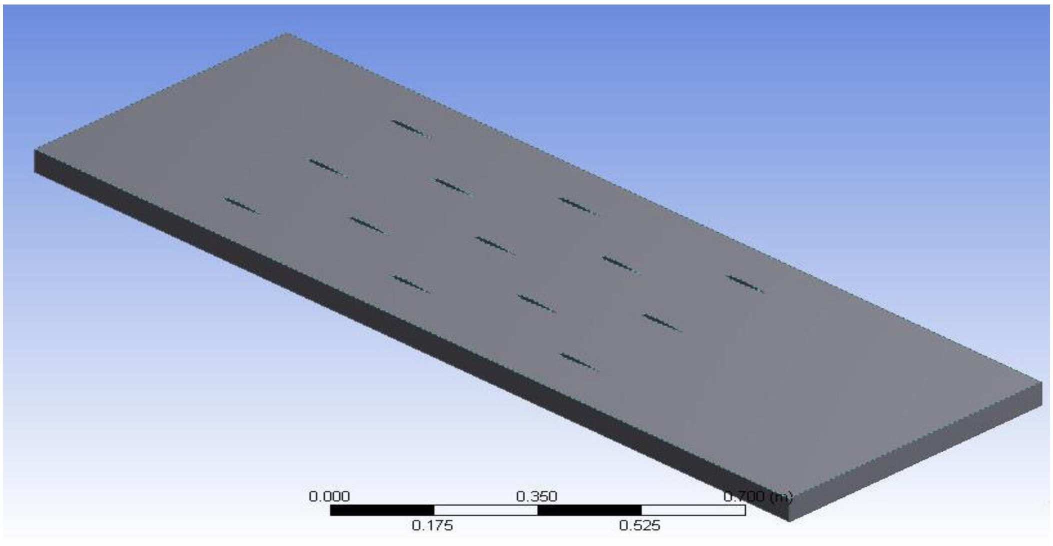

Figure 9: Model with Staggered NACA Airfoil Fins (10cm)

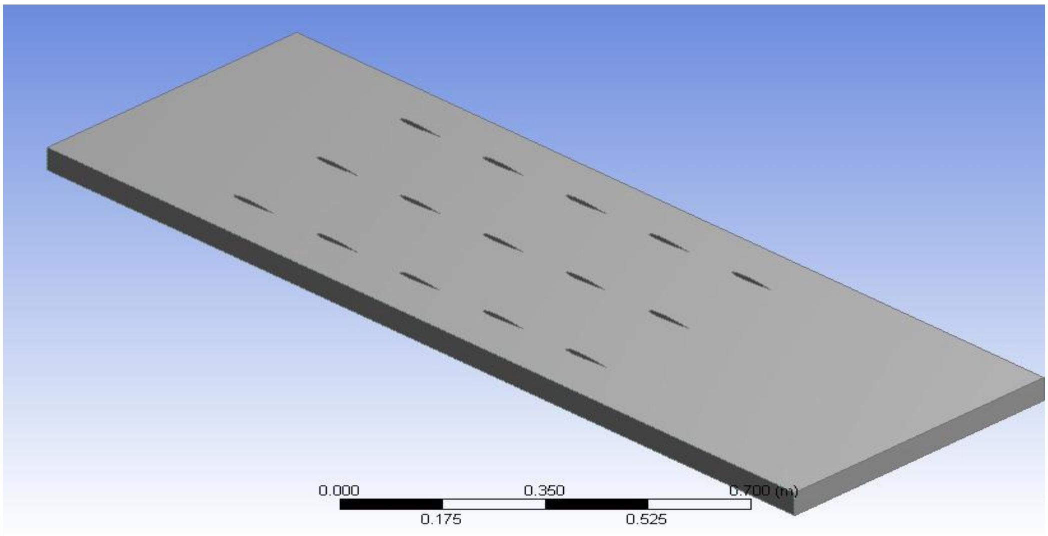

Figure 10: Model with Horizontal NACA Airfoil Fins (10cm)

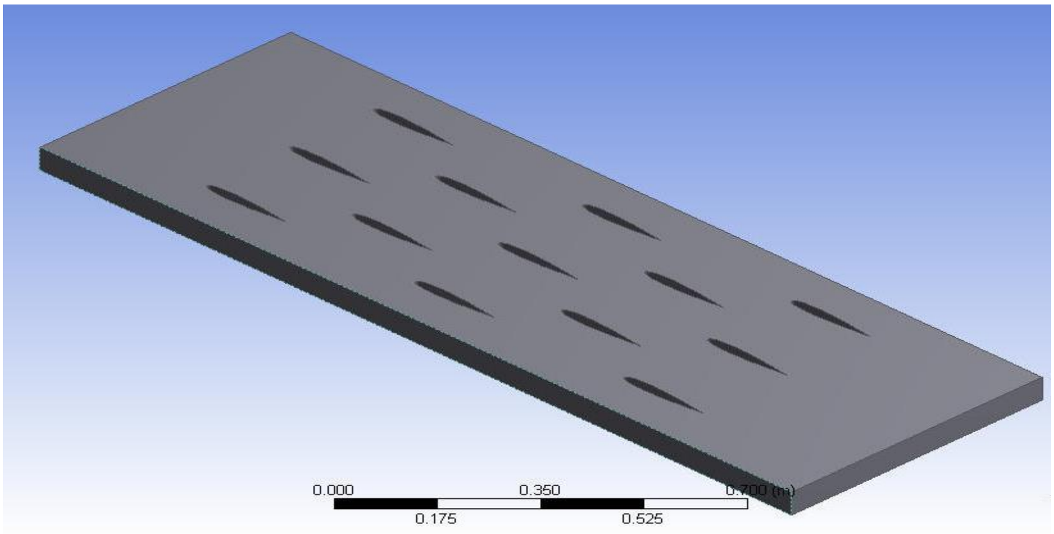

Figure 11: Model with Staggered NACA Airfoil Fins (20cm)

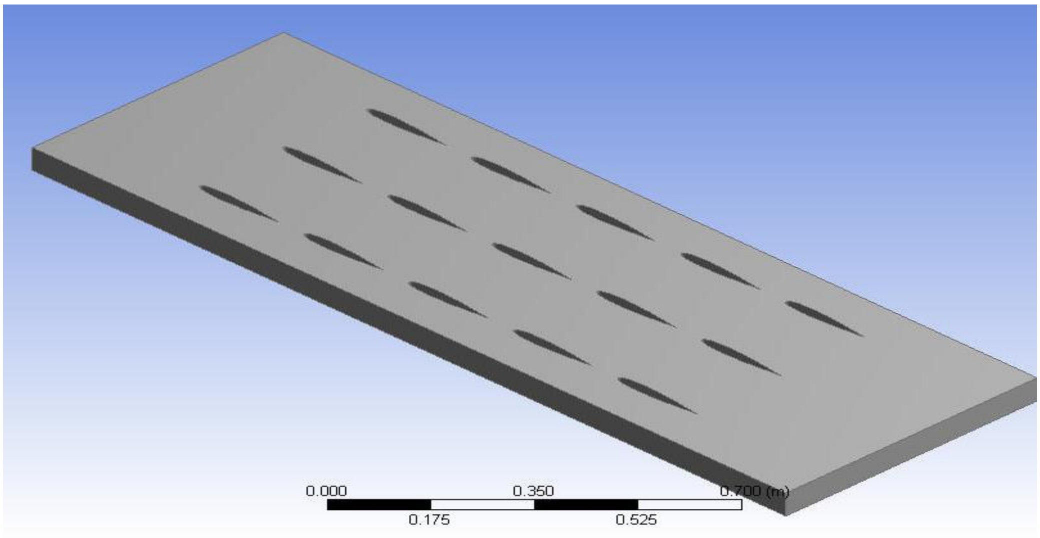

Figure 12: Model with Horizontal NACA Airfoil Fins (20cm)

3.3 Project Flow Chart

Below is the flow chart that shows the flowing progress of my final year report.

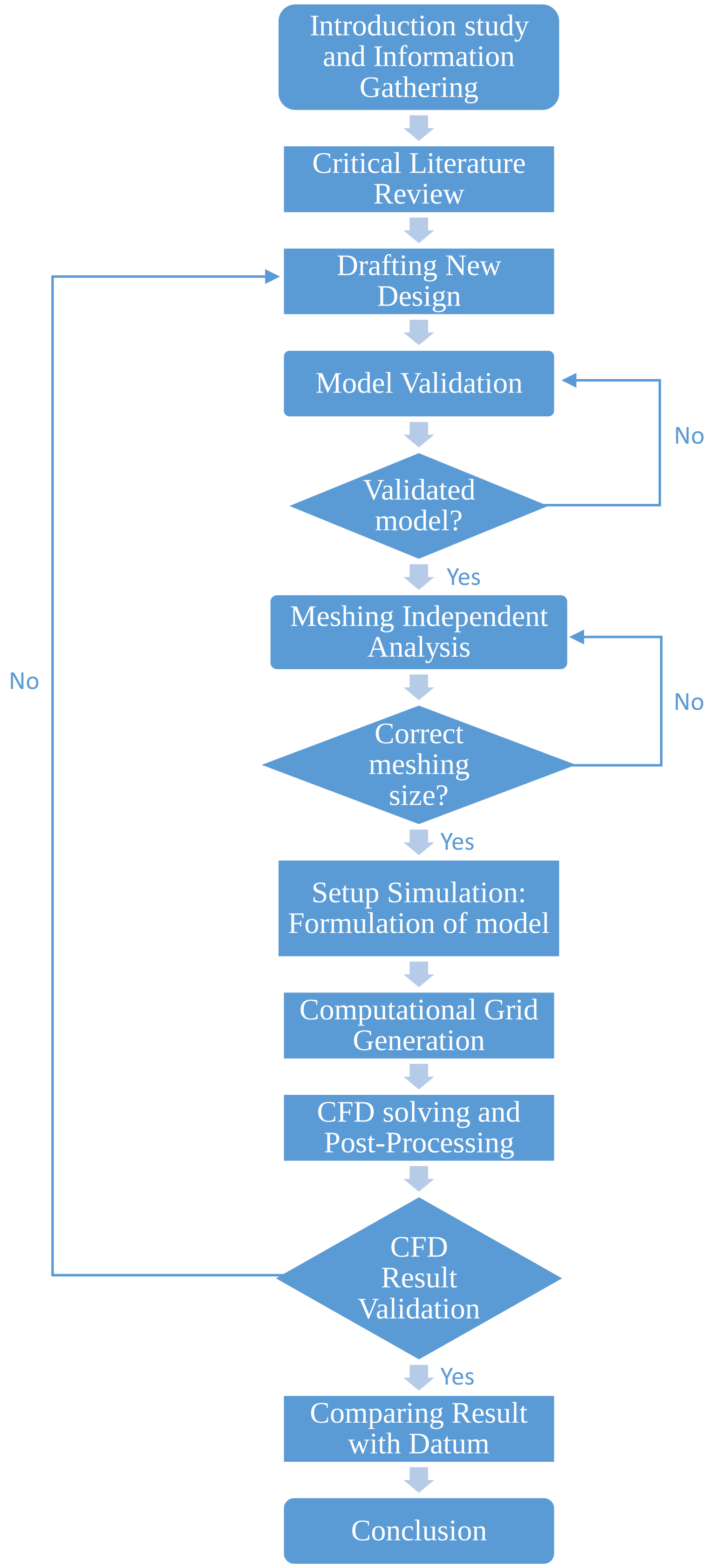

Figure 13: Flow Chart: Process Flow for FYP 1 and 2

3.4 Key Milestones

In order to ensure that the project goes well and smooth, I have identified key milestones for my Final Year Project 1. Figure below shows the summarize key milestones for both Final Year Project:

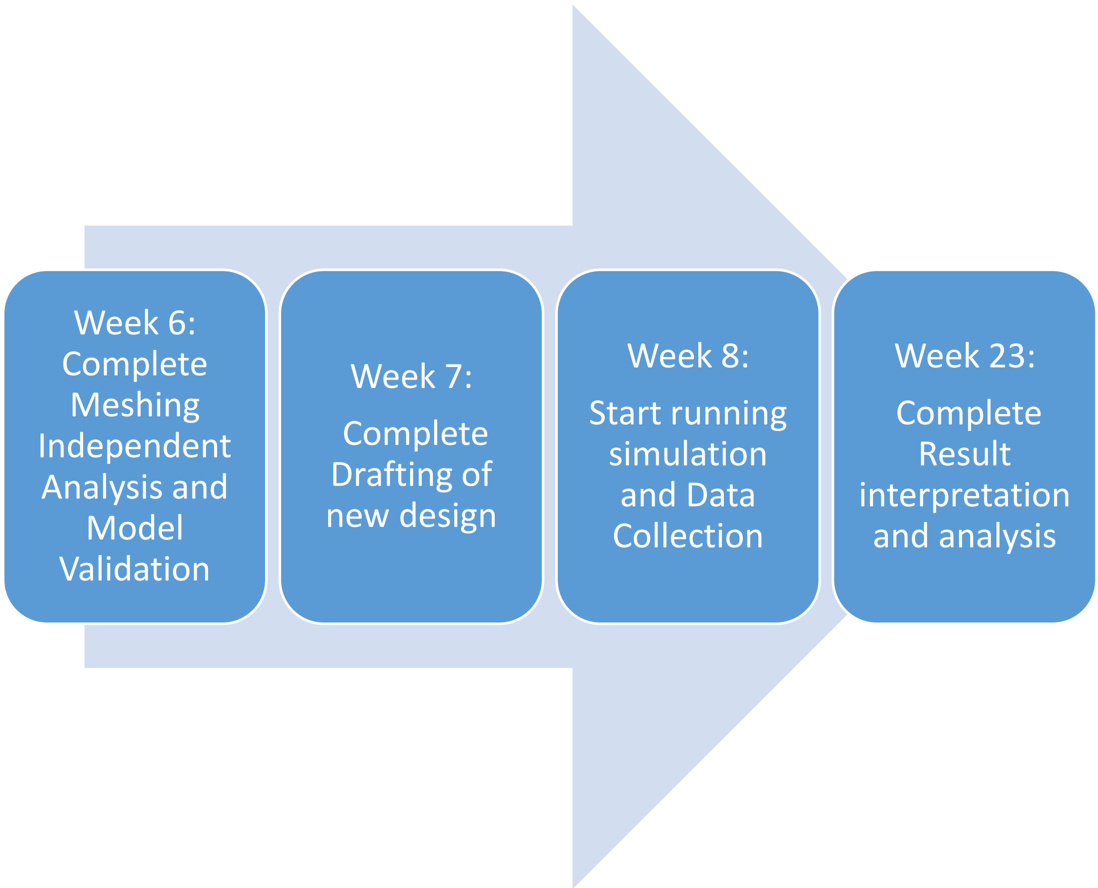

Figure 14: Key Milestones for FYP 1 and 2

3.5 Gantt-Chart

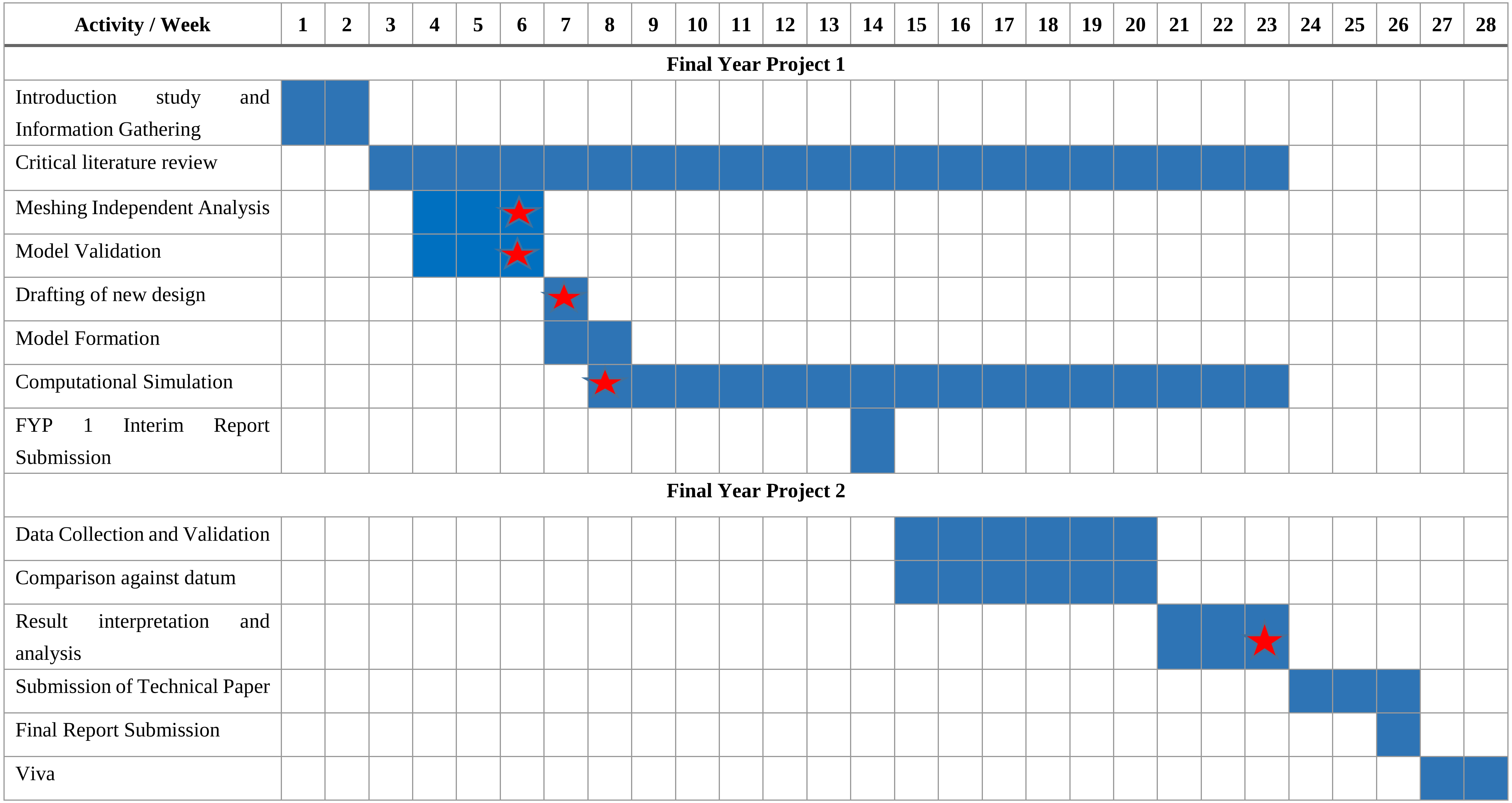

Figure 15: Gantt Chart for FYP 1 & 2

CHAPTER 4: RESULT AND DISCUSSION

4.1 Results from simulation

Every model went through the simulation with the same boundary conditions so that the results collected are consistent enough to be compared among each other. Simulations are running in 6 different values of Reynolds number in order to see the trend of the results: starting from Re = 10000 to Re = 15000. By using the Reynolds number equation, we can calculate exact value of inlet velocity we should use for the simulation. After calculation, the inlet velocity for each Reynolds number equals to:

Table 5: Value for Inlet Velocity with respect to Reynolds Number

Reynolds Number	Inlet velocity, m/s
10000	1.3390
11000	1.4729
12000	1.6808
13000	1.7407
14000	1.8746
15000	2.0085

i. Datum

After running the simulation on the Datum, which is the model that does not consist of any fins in it, this is the result obtained:

Table 6: Results for Temperature vs Reynolds Number (Datum)

Re	Velocity (m/s)	flux	Total temperature inlet (K)	Total temperature outlet (K)	Total temperature difference (K)
10000	1.339	1000	300.05	319.26	19.21
11000	1.472	1000	300.04	317.53	17.49
12000	1.606	1000	300.04	316.09	16.05
13000	1.740	1000	300.04	314.87	14.83
14000	1.874	1000	300.04	313.82	13.78
15000	2.008	1000	300.03	312.91	12.88

Table 7: Results for Pressure vs Reynolds Number (Datum)

Re	Velocity (m/s)	flux	Total Pressure inlet (Pa)	Total Pressure outlet (Pa)	Total Pressure difference (Pa)
10000	1.339	1000	1.741	1.123	0.618
11000	1.472	1000	2.086	1.358	0.728
12000	1.606	1000	2.460	1.616	0.844
13000	1.740	1000	2.865	1.896	0.969
14000	1.874	1000	3.299	2.198	1.101
15000	2.008	1000	3.764	2.523	1.241

From table 6 and 7, we can observe that the temperature difference between inlet and outlet decreases when the velocity increases. This trend is logic as we know that when the inlet velocity increases, the time taken for the air to flow through solar air heater will be shorter and lesser, causing shorter time for heat transfer to take place and lesser heat to be transferred to the air from the absorber plate. As for pressure, we can see that the pressure decreases from inlet to outlet, which indicates energy losses due to friction between the air and the solar air heater. According to continuity equation, we know that if the area of the inlet and outlet remains the same, the velocity will remain the same. However, due to the increase shear force between air and wall of solar air heater, the velocity tends to decrease due to friction force. Therefore, pressure acts the role of converting its energy to kinetic energy in order to maintain the flow velocity. Thus, when the inlet velocity increases, the pressure drop increases. Below show contour images produced from the simulation:

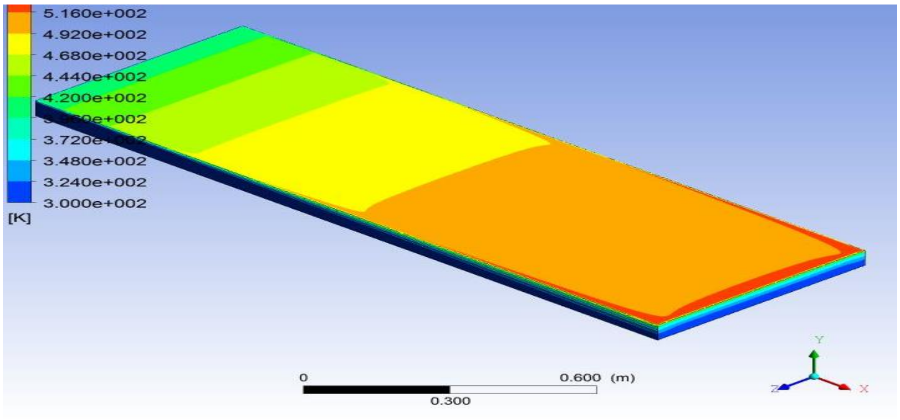

Figure 16: Contour Image that shows Temperature distribution (Datum)

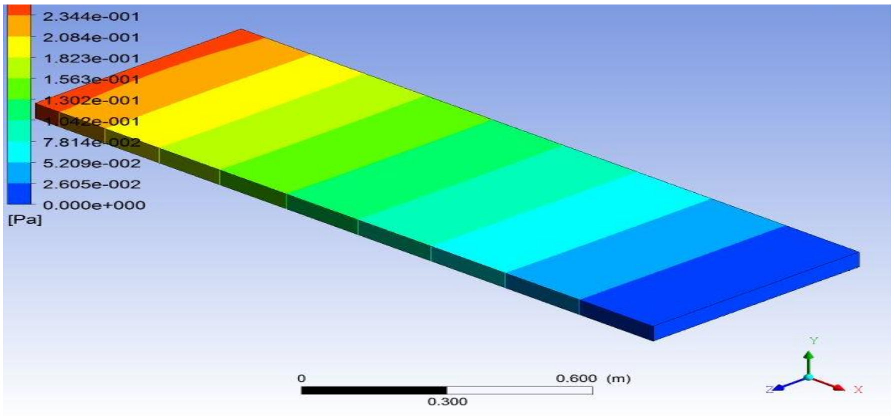

Figure 17: Contour Image that shows Pressure Distribution (Datum)

ii. Solar Air Heater with NACA Airfoil shaped fins

A. Horizontal Arrangement

The same procedure of simulation was used onto the models with horizontal arrangement of NACA Airfoil shaped fins. Below are the results produced from the simulation:

1. 5cm NACA Airfoil fins:

Table 8: Results for Temperature vs Reynolds Number (Horizontal [5cm])

Re	Velocity (m/s)	flux	Temperature inlet (K)	Temperature outlet (K)	Total temperature difference (K)
10000	1.339	1000	300.05	319.28	19.23
11000	1.473	1000	300.05	317.56	17.51
12000	1.607	1000	300.04	316.11	16.06
13000	1.741	1000	300.04	314.89	14.85
14000	1.875	1000	300.04	313.84	13.81
15000	2.009	1000	300.03	312.93	12.90

Table 9: Results for Pressure vs Reynolds Number (Horizontal [5cm])

Re	Velocity (m/s)	flux	Total Pressure inlet (Pa)	Total Pressure outlet (Pa)	Total Pressure difference (Pa)
10000	1.339	1000	1.808	1.123	0.686
11000	1.473	1000	2.165	1.358	0.807
12000	1.607	1000	2.552	1.615	0.937
13000	1.741	1000	2.971	1.895	1.076
14000	1.875	1000	3.421	2.197	1.223
15000	2.009	1000	3.901	2.522	1.379

2. 10cm NACA Airfoil fins:

Table 10: Results for Temperature vs Reynolds Number (Horizontal [10cm])

Re	Velocity (m/s)	flux	Temperature inlet (K)	Temperature outlet (K)	Total temperature difference (K)
10000	1.339	1000	300.05	319.07	19.01
11000	1.473	1000	300.05	317.38	17.33
12000	1.607	1000	300.04	315.94	15.90
13000	1.741	1000	300.04	314.74	14.69
14000	1.875	1000	300.04	313.70	13.67
15000	2.009	1000	300.03	312.83	12.79

Table 11: Results for Pressure vs Reynolds Number (Horizontal [10cm])

Re	Velocity (m/s)	flux	Total Pressure inlet (Pa)	Total Pressure outlet (Pa)	Total Pressure difference (Pa)
10000	1.339	1000	1.856	1.122	0.733
11000	1.473	1000	2.223	1.357	0.865
12000	1.607	1000	2.619	1.615	1.004
13000	1.741	1000	3.048	1.895	1.153
14000	1.875	1000	3.508	2.197	1.311
15000	2.009	1000	4.007	2.519	1.487

3. 20cm NACA Airfoil fins:

Table 12: Results for Temperature vs Reynolds Number (Horizontal [20cm])

Re	Velocity (m/s)	flux	Temperature inlet (K)	Temperature outlet (K)	Total temperature difference (K)
10000	1.339	1000	300.05	318.41	18.36
11000	1.473	1000	300.05	316.78	16.73
12000	1.607	1000	300.04	315.42	15.38
13000	1.741	1000	300.04	314.22	14.18
14000	1.875	1000	300.03	313.24	13.20
15000	2.009	1000	300.03	312.36	12.33

Table 13: Results for Pressure vs Reynolds Number (Horizontal [20cm])

Re	Velocity (m/s)	flux	Total Pressure inlet (Pa)	Total Pressure outlet (Pa)	Total Pressure difference (Pa)
10000	1.339	1000	1.983	1.124	0.859
11000	1.473	1000	2.373	1.359	1.014
12000	1.607	1000	2.797	1.617	1.180
13000	1.741	1000	3.247	1.898	1.349
14000	1.875	1000	3.739	2.200	1.540
15000	2.009	1000	4.259	2.525	1.734

From table 8 to 13, we can see that both temperature difference and pressure drop shows the same trend as the one obtained from Datum: when the inlet velocity increases, the total temperature difference decreases due to shorter heat transfer duration between air and absorber plate; and increase in pressure difference which indicates more energy losses due to the increase of shear force.

By comparing between models with different fin size, we can see that model with 5cm NACA Airfoil fins has a highest temperature difference among all, which indicates that it has the highest rate of heat transfer among all. By looking at the pressure drop, 5cm fin model has the lowest pressure drop among all, which means having the least energy losses compare to the other 2 models. From here, we can come up with a conclusion: For models with horizontal arrangement NACA Airfoil fins, 5cm fin size model shows the best result for both heat transfer and pressure drop.

Below are contour images for horizontal arrangement models produced by ANSYS Simulation:

i. Model with 5cm fins:

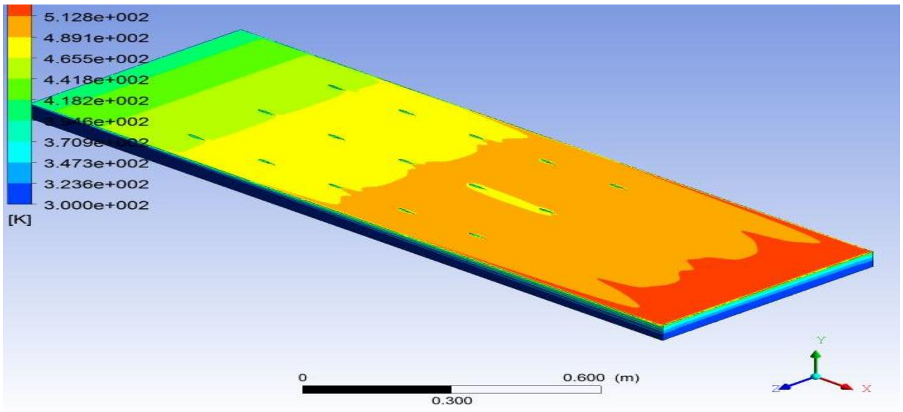

Figure 18: Contour Image (Total Temperature distribution)

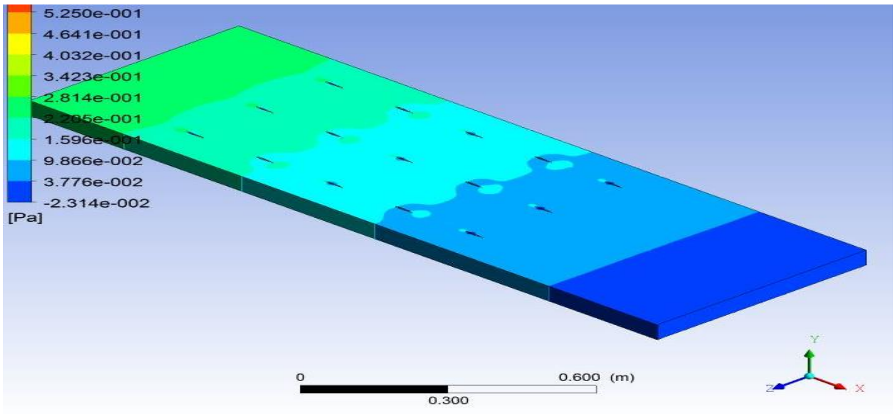

Figure 19: Contour Image (Total Pressure distribution)

ii. Model with 10cm fins:

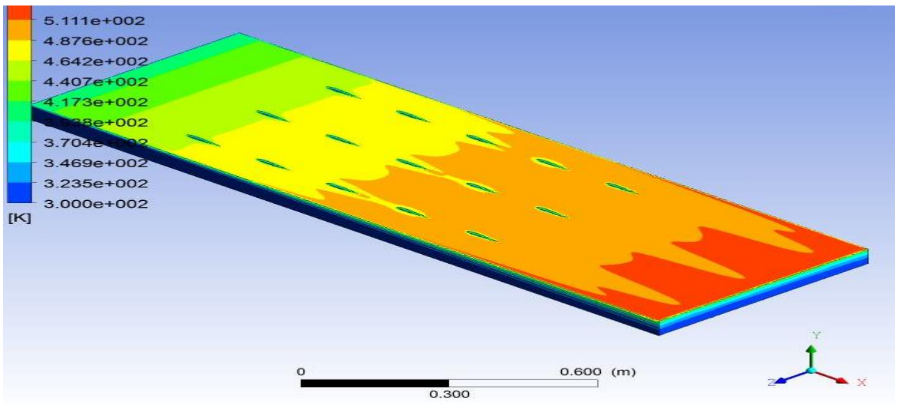

Figure 20: Contour Image (Total Temperature distribution)

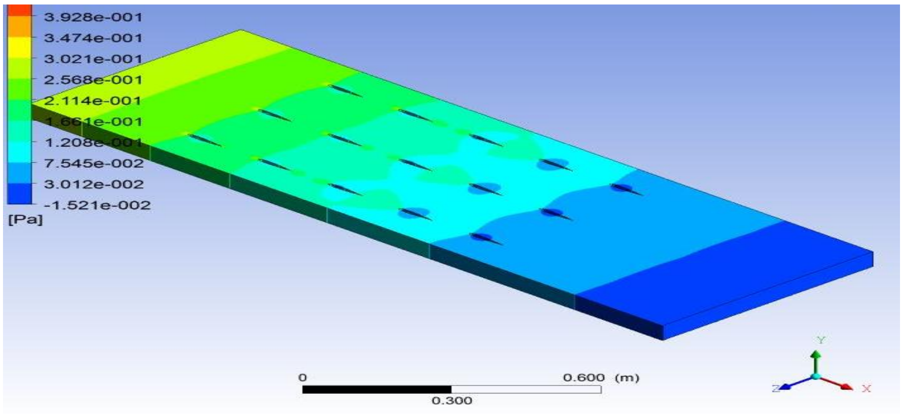

Figure 21: Contour Image (Total Pressure distribution)

iii. Model with 20cm fins:

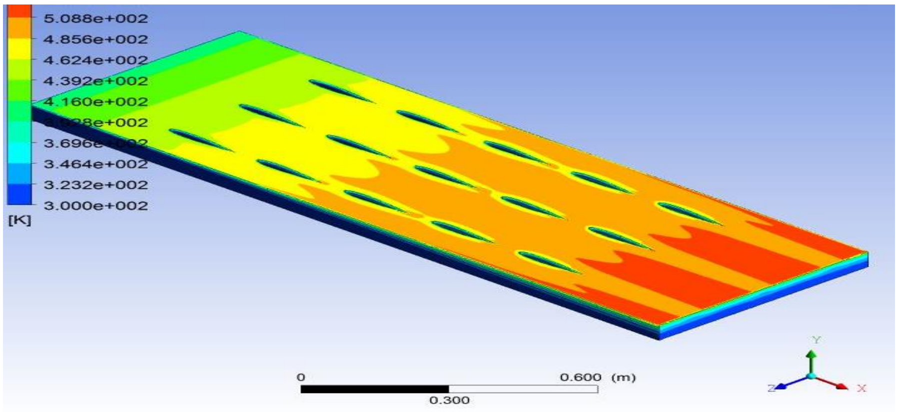

Figure 22: Contour Image (Total Temperature distribution)

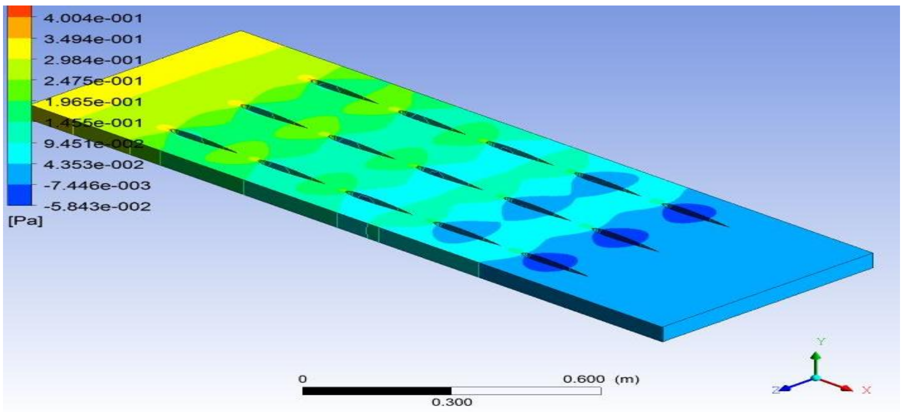

Figure 23: Contour Image (Total Pressure distribution)

B. Staggered Arrangement:

Same for staggered arrangement, there are 3 models with different size of fins: 5cm, 10cm and 20cm. Same procedure is applied to all 3 of the models. Below are the results obtained from ANSYS simulation:

1. 5cm NACA Airfoil fins:

Table 14: Results for Temperature vs Reynolds Number (Staggered [5cm])

Re	Velocity (m/s)	flux	Temperature inlet (K)	Temperature outlet (K)	Total temperature difference (K)
10000	1.339	1000	300.05	319.29	19.23
11000	1.473	1000	300.05	317.57	17.52
12000	1.607	1000	300.04	316.12	16.08
13000	1.741	1000	300.04	314.89	14.85
14000	1.875	1000	300.04	313.85	13.81
15000	2.009	1000	300.04	312.93	12.90

Table 15: Results for Pressure vs Reynolds Number (Staggered [5cm])

Re	Velocity (m/s)	flux	Total Pressure inlet (Pa)	Total Pressure outlet (Pa)	Total Pressure difference (Pa)
10000	1.339	1000	1.063	0.387	0.676
11000	1.473	1000	1.289	0.492	0.796
12000	1.607	1000	1.534	0.610	0.924
13000	1.741	1000	1.802	0.742	1.060
14000	1.875	1000	2.095	0.890	1.206
15000	2.009	1000	2.406	1.049	1.357

2. 10cm NACA Airfoil fins:

Table 16: Results for Temperature vs Reynolds Number (Staggered [10cm])

Re	Velocity (m/s)	flux	Temperature inlet (K)	Temperature outlet (K)	Total temperature difference (K)
10000	1.339	1000	300.05	319.16	19.11
11000	1.473	1000	300.05	317.44	17.39
12000	1.607	1000	300.04	316.01	15.96
13000	1.741	1000	300.04	314.79	14.75
14000	1.875	1000	300.04	313.75	13.71
15000	2.009	1000	300.03	312.84	12.81

Table 17: Results for Pressure vs Reynolds Number (Staggered [10cm])

Re	Velocity (m/s)	flux	Total Pressure inlet (Pa)	Total Pressure outlet (Pa)	Total Pressure difference (Pa)
10000	1.339	1000	1.847	1.122	0.725
11000	1.473	1000	2.210	1.357	0.853
12000	1.607	1000	2.605	1.614	0.991
13000	1.741	1000	3.032	1.894	1.138
14000	1.875	1000	3.489	2.196	1.292
15000	2.009	1000	3.977	2.521	1.457

3. 20cm NACA Airfoil fins:

Table 18: Results for Temperature vs Reynolds Number (Staggered [20cm])

Re	Velocity (m/s)	flux	Temperature inlet (K)	Temperature outlet (K)	Total temperature difference (K)
10000	1.339	1000	300.05	318.56	18.51
11000	1.473	1000	300.05	316.89	16.84
12000	1.607	1000	300.04	315.49	15.45
13000	1.741	1000	300.04	314.32	14.28
14000	1.875	1000	300.04	313.31	13.27
15000	2.009	1000	300.03	312.44	12.40

Table 19: Results for Pressure vs Reynolds Number (Staggered [20cm])

Re	Velocity (m/s)	flux	Total Pressure inlet (Pa)	Total Pressure outlet (Pa)	Total Pressure difference (Pa)
10000	1.339	1000	1.982	1.123	0.859
11000	1.473	1000	2.370	1.359	1.011
12000	1.607	1000	2.791	1.617	1.174
13000	1.741	1000	3.245	1.897	1.348
14000	1.875	1000	3.734	2.199	1.534
15000	2.009	1000	4.253	2.524	1.729

From table 14 to 19, it was found out that the trend for the temperature changes and pressure drop remains the same as Datum and models with horizontal arrangement. Model with 5cm NACA Airfoil fins has the highest temperature difference and lowest pressure drop among all, which indicates the highest rate of heat transfer and the least energy losses among the other models. This result is the same with models having horizontal arrangement fins, which leads us to a conclusion: disregarding the arrangement issue, the size of the fins has the biggest influence for rate of heat transfer and pressure drop:

1. Smaller the size of the fins increase the area for heat transfer between air and absorber plate, which leads to higher temperature change.
2. Smaller size fins reduce the amount of shear friction between the air and the wall, causing lower pressure drop and lesser energy losses.

Below are contour images for horizontal arrangement models produced by simulation:

i. Model with 5cm fins:

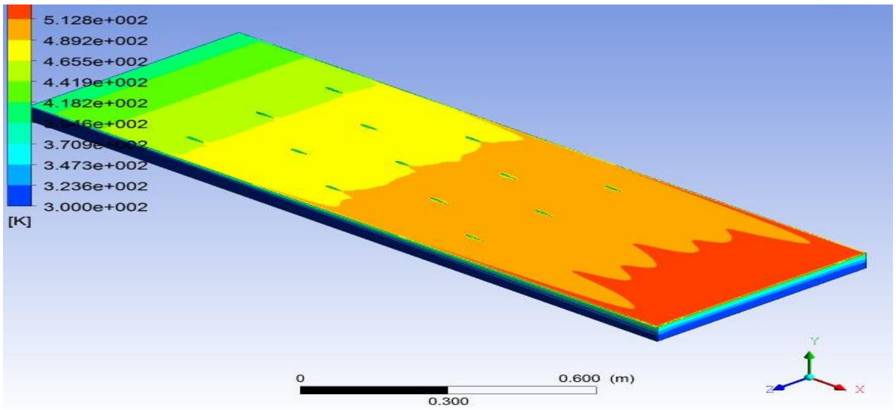

Figure 24: Contour Image (Total Temperature distribution)

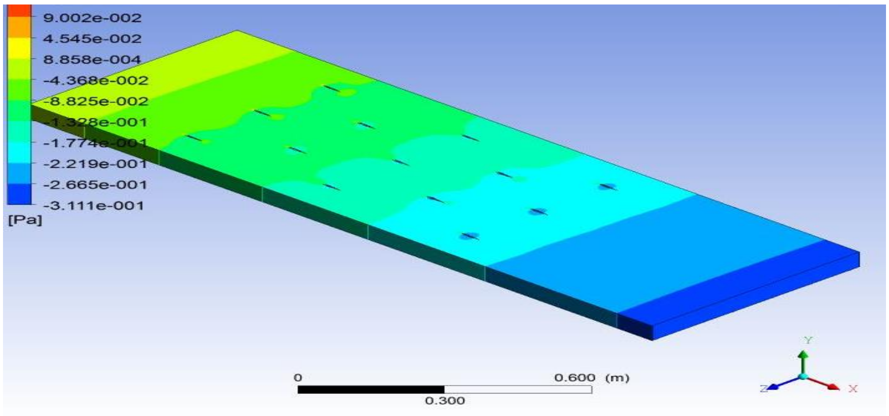

Figure 25: Contour Image (Total Pressure distribution)

ii. Model with 10cm fins:

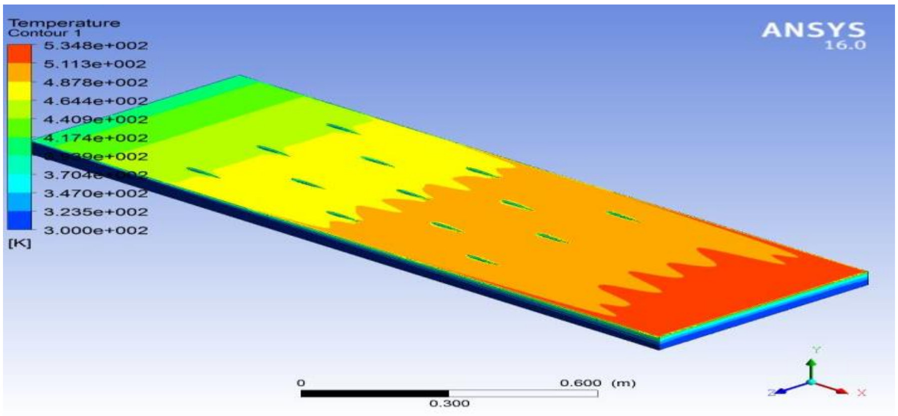

Figure 26: Contour Image (Total Temperature distribution)

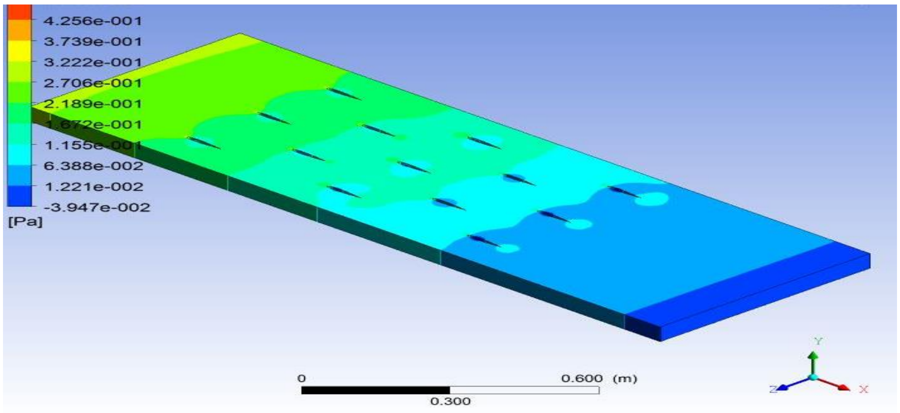

Figure 27: Contour Image (Total Pressure distribution)

iii. Model with 20cm fins:

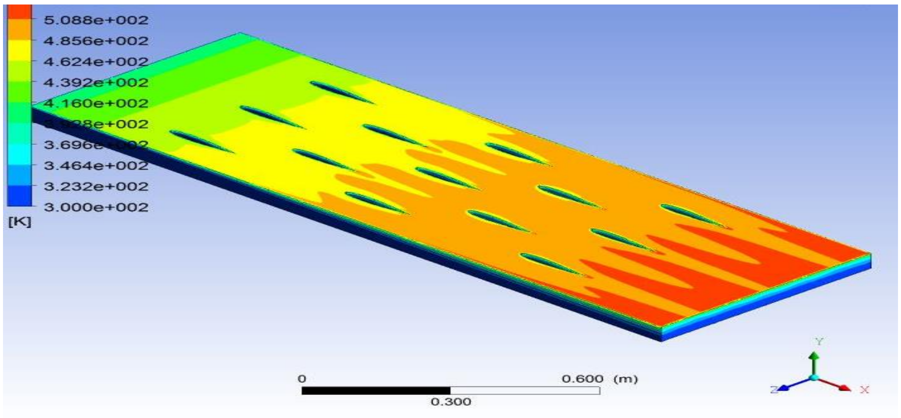

Figure 28: Contour Image (Total Temperature distribution)

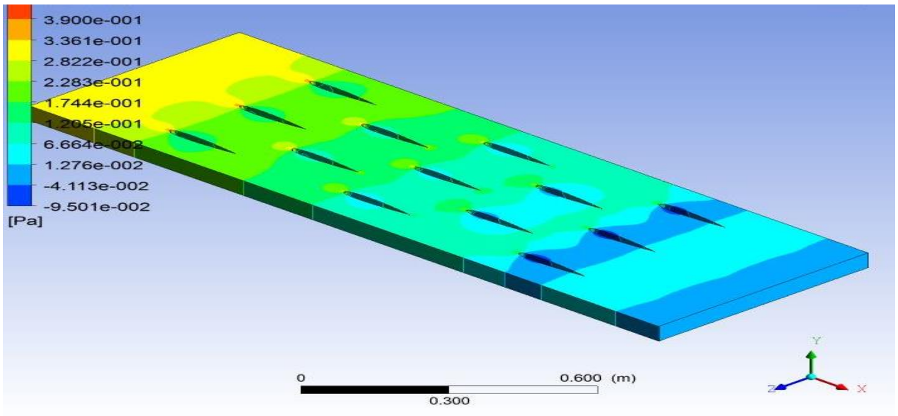

Figure 29: Contour Image (Total Pressure distribution)

4.4 Comparing Datum and models with Staggered and Horizontal arrangement

The main objective for this project is to study the effect of NACA Airfoil fins in improving the performance of solar air heater. In order to analyze the effect of the additional fins on the performance, comparisons are done between datum with all of the other models with fins according to the results obtained from the simulation.

Below are graphs that compares the temperature difference and pressure drop for each model:

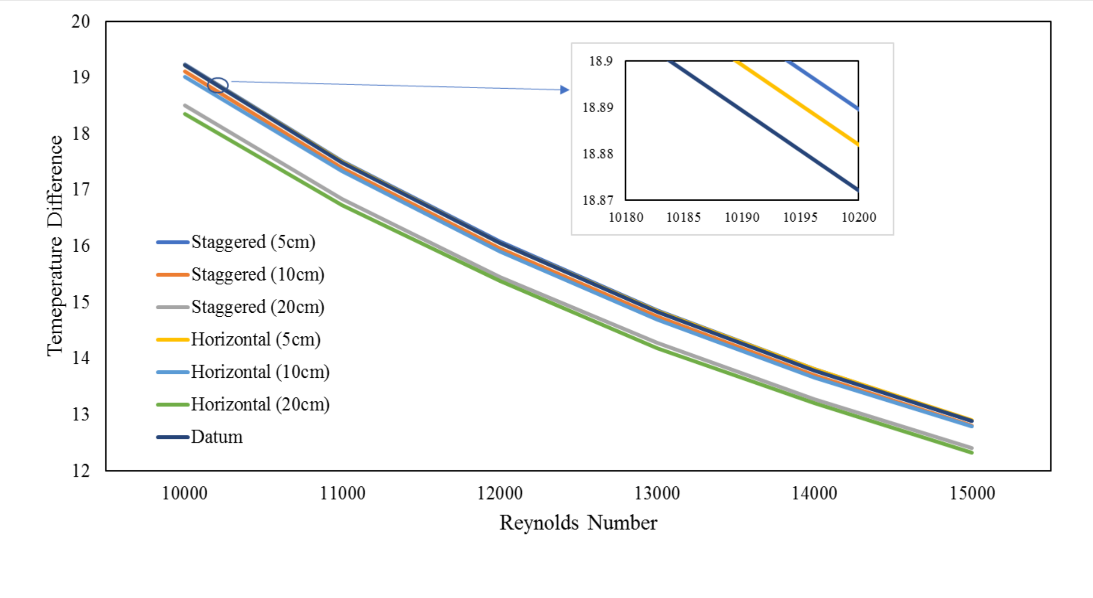

Figure 30: Graph Temperature Difference vs Reynolds Number

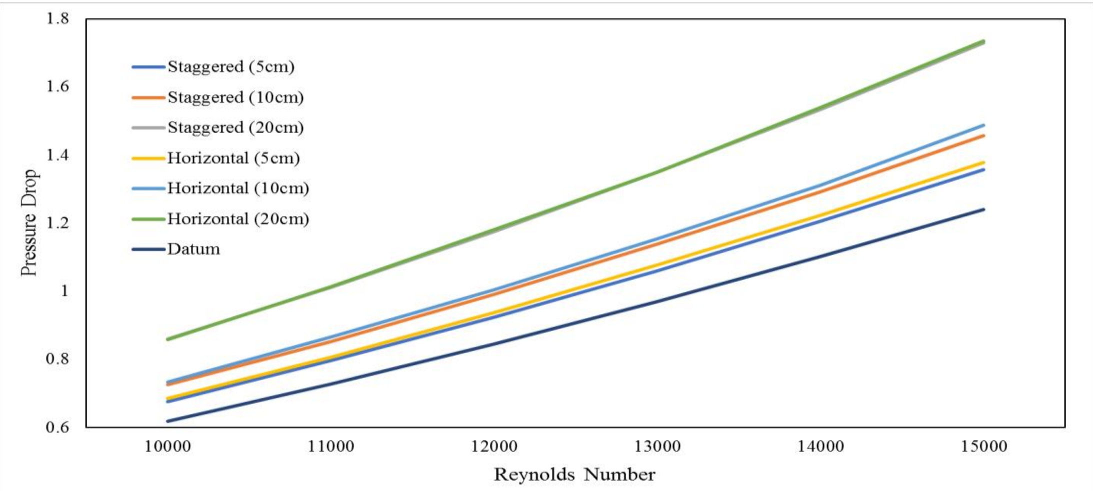

Figure 31: Graph Pressure Drop vs Reynolds Number

By looking at the graphs produced from the results obtained from the simulation, we notice that model with 5cm staggered arrangement fins has the highest temperature difference among all models and a little bit more than datum, which shows that this model has the highest thermal efficiency among all model. As for pressure drop, datum has the lowest pressure drop among all of the others, following by model with 5cm staggered arrangement fins. By judging according to the graph above, model with 5cm staggered arrangement fins will be the only model that has the effect on improving the thermal performance of solar air heater, but with the term of sacrificing more energy losses.

In order to justify which model has the best potential in enhancing the overall performance of solar air heater, calculation for thermal-hydraulic performance is applied to every single model with fins. To calculate thermal-hydraulic performance, calculation for ratio of Nusselt mumber and hydraulic performance were done separately beforehand.

i. Nusselt Number ratio

Nusselt Number for each model is calculated by using the formula:

$$Nu = (h * D_h)/k \tag{12}$$

Where : h = Convective heat transfer coefficient

D_h = Hydraulic Diameter

k = Conductive heat transfer coefficient

After running the simulation for each model, the values and results obtained from the simulation are used to calculate convective heat transfer coefficient by using the formula:

$$h = \frac{Q}{A_c * (T_{hs} - T_{ave})} \tag{13}$$

where : Q = Useful energy gained

A_c= Area of heat transfer

T_{hs}= Temperature of Heat Source

T_{ave}= Average temperature of working fluid (Air)

Useful energy gained, Q can be calculated by using the formula:

$$Q = \dot{m} * C_p * (T_{out} - T_{in}) \quad (14)$$

Where : $\dot{m}$ = mass flow rate

C_p= specific heat of air (J/kg K)

Below shows an example of the results obtained from the calculation for useful energy gained and Nusselt number for model with 5cm staggered arrangement fins , and also table consists of Nusselt Number for every model with fins:

Table 20: Calculation for Q (Model with 5cm fins: Staggered)

Re	Mass flow rate (kg/s)	Temperature inlet (K)	Temperature outlet (K)	Average Temperature (K)	Heat Source Temperature (K)	Q
10000	0.0590	300.05	319.29	309.67	347.04	1135.67
11000	0.0650	300.05	317.57	308.81	343.37	1137.93
12000	0.0709	300.04	316.12	308.08	340.23	1139.44
13000	0.0768	300.04	314.89	307.47	337.50	1140.20
14000	0.0827	300.04	313.85	306.94	335.18	1141.91
15000	0.0886	300.04	312.93	306.48	333.08	1142.23

Table 21: Calculation for Nusselt Number (Model with 5cm fins: Staggered)

Re	Q (W)	Heat Source Area (m^2)	h $W/(m^2K)$	D_h (m)	k $W/(m^2K)$	Nu
10000	1135.67	1.08	28.14	0.1091	0.024	127.90
11000	1137.93	1.08	30.48	0.1091	0.024	138.56
12000	1139.44	1.08	32.82	0.1091	0.024	149.17
13000	1140.20	1.08	35.15	0.1091	0.024	159.78
14000	1141.91	1.08	37.45	0.1091	0.024	170.24
15000	1142.23	1.08	39.76	0.1091	0.024	180.73

Table 22: Results for Nusselt Number against Reynolds Number

Nusselt Number						
Re	Staggered			Horizontal		
	5cm	10cm	20cm	5cm	10cm	20cm
10000	127.90	128.03	129.42	127.97	129.09	131.04
11000	138.56	138.76	140.35	138.63	139.65	141.69
12000	149.17	149.36	151.14	149.28	150.43	152.08
13000	159.78	159.92	161.79	159.78	161.02	163.70
14000	170.24	170.47	172.39	170.26	171.49	173.96
15000	180.73	180.92	182.92	180.69	181.24	184.74

After getting the Nusselt number for each model, the values are used to calculate Nusselt Number ratio by simply dividing them with the Nusselt number for datum. Table below shows the values for Nusselt number ratio for a specific value of Reynolds number and the graph Nusselt number ratio with respect of Reynolds number:

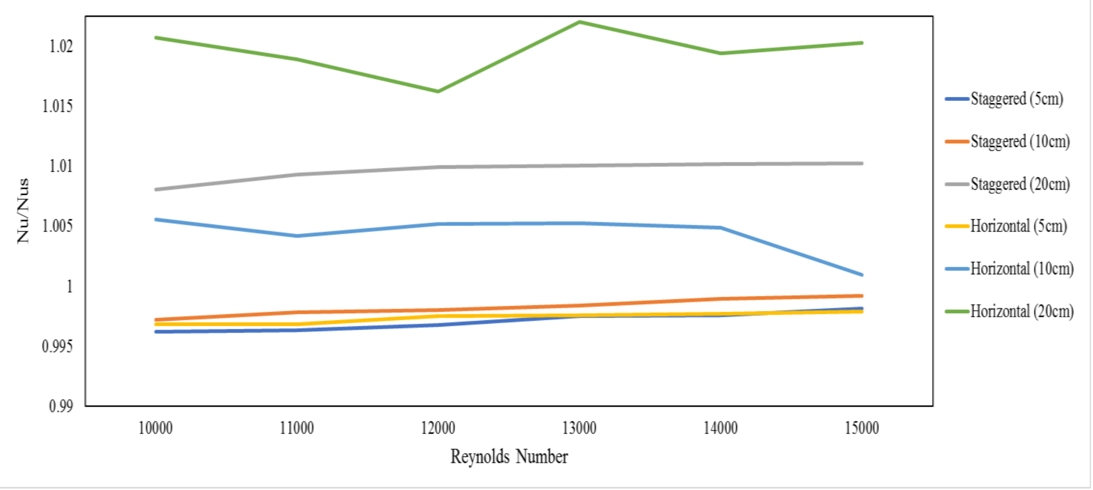

Figure 32: Graph Nusselt Number ratio vs Reynolds Number

Table 23: Results for Nusselt Number ratio against Reynolds Number

Nusselt Number Ratio						
Re	Staggered			Horizontal		
	5cm	10cm	20cm	5cm	10cm	20cm
10000	0.9962	0.9973	1.008	0.9968	1.006	1.021
11000	0.9964	0.9979	1.009	0.9969	1.004	1.019
12000	0.9968	0.9981	1.010	0.9975	1.005	1.016
13000	0.9975	0.9984	1.010	0.9976	1.005	1.022
14000	0.9976	0.9989	1.010	0.9977	1.005	1.019
15000	0.9982	0.9992	1.010	0.9979	1.001	1.020

The graph above shows that model with 20cm horizontal arrangement fins has the highest value of Nusselt number ratio among all of the others due to having the highest Nusselt number among all of the models.

ii. Friction Factor Ratio

Friction factor ratio is the ratio between friction factor of models against friction factor of datum. After running the simulation, the inlet and outlet pressure can be obtained for each of the models. Therefore, by using this information and apply to the formula below, we will get the value of friction factor for each of the model at a certain Reynolds number:

$$f = \frac{\Delta PD}{2\rho l v^2} \tag{15}$$

Where : f = fanning friction factor

$\Delta P =$ pressure difference between inlet and outlet, Pa

D = Hydraulic diameter / Characteristic length, m

$\rho =$ density of working fluid (air), kg/m^3

$l =$ total length of duct, m

$v =$ inlet velocity, m/s

Below shows an example of the results obtained from the calculation of friction factor for model with 5cm staggered arrangement fins, and also table consists of friction factor for every model with fins:

Table 24: Calculation of Friction Factor (model with 5cm fins: Staggered)

Total Pressure inlet (Pa)	Total Pressure outlet (Pa)	Pressure difference	D_h (m)	Density kg/m^3	Duct Length (m)	inlet velocity (m/s)	friction factor
0.5267	0.2847	0.2420	0.1091	1.225	1.8	0.670	0.0134
0.3767	0.0603	0.3165	0.1091	1.225	1.8	0.803	0.0121
0.5159	0.1348	0.3811	0.1091	1.225	1.8	0.937	0.0107
0.6770	0.2125	0.4644	0.1091	1.225	1.8	1.071	0.0100
0.8594	0.2927	0.5667	0.1091	1.225	1.8	1.205	0.0097
1.0632	0.3867	0.6765	0.1091	1.225	1.8	1.339	0.0093

Table 25: Results for Friction factor

Friction Factor						
Re	Staggered			Horizontal		
	5cm	10cm	20cm	5cm	10cm	20cm
10000	0.0093	0.0100	0.0119	0.0095	0.0101	0.0119
11000	0.0091	0.0097	0.0115	0.0092	0.0099	0.0116
12000	0.0089	0.0095	0.0113	0.0090	0.0096	0.0113
13000	0.0087	0.0093	0.0110	0.0088	0.0094	0.0110
14000	0.0085	0.0091	0.0108	0.0086	0.0092	0.0108
15000	0.0083	0.0089	0.0106	0.0085	0.0091	0.0106

From here, we notice that model with 5cm staggered arrangement fins has the lowest value friction factor while model with 20cm horizontal arrangement fins has the highest value of friction factor. This indicates that 5cm staggered arrangement fins' model experience the least pressure drop while 20cm staggered arrangement fins' model suffers the most pressure drop. Pressure drop is another way of indicating energy losses, therefore the smaller the value of friction factor, the lesser energy loss occurs. For this scenario, model with 5cm staggered arrangement fins is the best model in minimizing energy loss.

After getting all the values of friction factor, friction factor ratio is calculated by dividing models' friction factor with datum's friction factor. A table and a graph are formed with the values of friction factor with respect to Reynolds number:

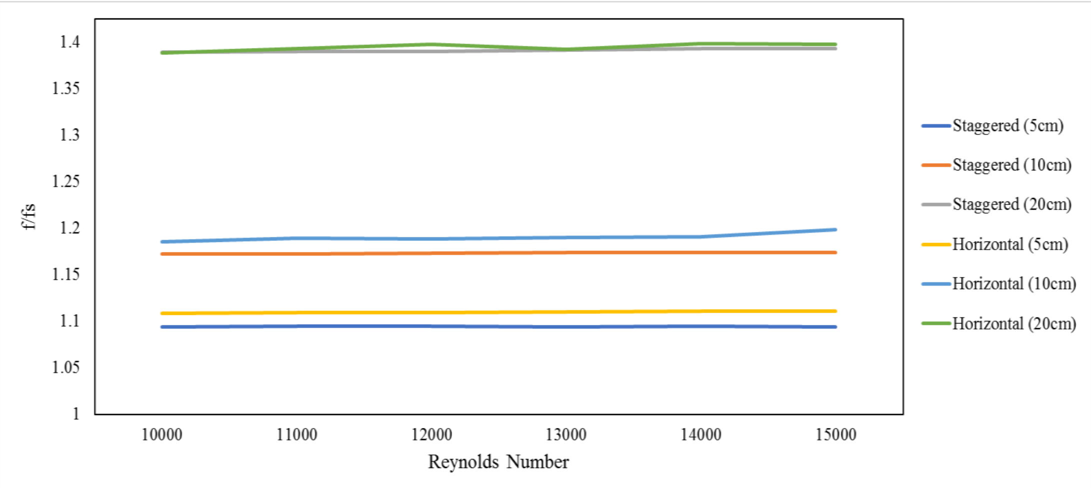

Figure 33: Graph Friction Factor ratio vs Reynolds Number

Table 26: Results for Friction Factor ratio against Reynolds Number

Friction Factor Ratio						
Re	Staggered			Horizontal		
	5cm	10cm	20cm	5cm	10cm	20cm
10000	1.094	1.173	1.389	1.109	1.186	1.389
11000	1.094	1.173	1.390	1.110	1.189	1.393
12000	1.095	1.173	1.390	1.109	1.189	1.398
13000	1.094	1.174	1.392	1.110	1.190	1.392
14000	1.095	1.174	1.393	1.111	1.191	1.398
15000	1.094	1.174	1.393	1.111	1.199	1.398

iii. Thermal-Hydraulic performance:

To choose which model has the highest overall efficiency, both thermal and hydraulic efficiency need to be taken in account. Therefore, after having the ratio for Nusselt number and Friction factor, both information is used to calculated the thermal-hydraulic performance index by using the formula:

$$Thermo - hydraulic\ Performance\ Index = \frac{Nu/Nu_s}{(\frac{f}{f_s})^{1/3}} \qquad (16)$$

Where : $Nu =$ Model's Nusselt number

$Nu_s =$ Datum's Nusselt number

$f =$ Model's Friction factor

$f =$ Datum's Friction factor

Below show the results for model's performance index with respect to Reynolds number:

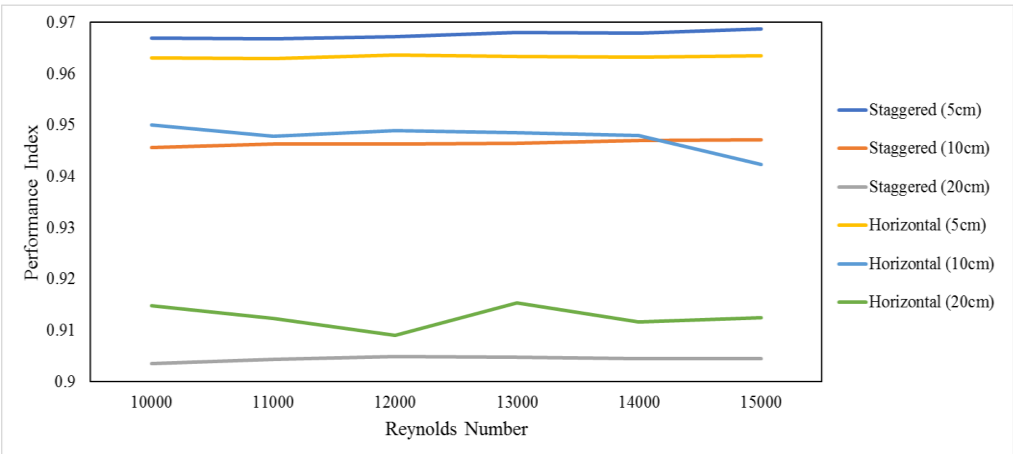

Figure 34: Graph Performance Index vs Reynolds Number

Table 27: Results for Performance Index against Reynolds Number

Performance Index						
Re	Staggered			Horizontal		
	5cm	10cm	20cm	5cm	10cm	20cm
10000	0.9670	0.9457	0.9035	0.9631	0.9501	0.9149
11000	0.9669	0.9463	0.9044	0.9629	0.9478	0.9123
12000	0.9673	0.9463	0.9049	0.9637	0.9490	0.9090
13000	0.9681	0.9465	0.9047	0.9633	0.9486	0.9153
14000	0.9679	0.9470	0.9044	0.9632	0.9480	0.9116
15000	0.9688	0.9472	0.9045	0.9635	0.9423	0.9125

By plotting the result against Reynolds number, we can clearly see that model with 5cm staggered arrangement fins has the highest overall efficiency, while model with 20cm staggered arrangement fins has the lowest overall efficiency among all.

If justification has been done separately for thermal and hydraulic performance, judgement may not be as convincing as for now. Model with 5cm staggered arrangement fins may have the worst hydraulic performance among others, but having the best thermal performance among all models. Therefore, after comparing both performance together, this model is still chosen being the model with best overall efficiency due to its high performance in thermal efficiency.

In a nutshell, we can conclude that thermal performance has much more impact that hydraulic performance in determining the overall efficiency of a solar air heater, and model with 5cm staggered arrangement fins is the best design that enhance the overall performance for solar air heater.

CHAPTER 5: CONCLUSION AND RECOMMENDATION

After analyzing all the results obtained from the simulation, a few conclusions can be made:

1. Investigation towards the effect of utilizing NACA Airfoil shape fins on the performance of solar air heater has been done:
   i. Model with NACA Airfoil shape fins has a higher rate of heat transfer due to the increase in heat transfer area; however, suffering in higher pressure drop due to the increase of shear friction between the working fluid and the wall of solar air heater.
2. Key parameters: size and arrangement of fins are investigated on the effect of them towards the performance of solar air heater:
   i. Model with 5cm NACA Airfoil fins has the highest overall performance: thermal-hydraulic performance due to lower pressure drop compare to models with other size fins. This is due to smaller size fins has a smaller contact area with the working fluid, reducing the shear friction force, which leads to decrease in pressure drop, higher thermal-hydraulic performance.
   ii. Model with staggered arrangement NACA Airfoil fins has a lower pressure drop comparing to horizontal arrangement models. This indicates a lower energy lost, which increase the thermal-hydraulic performance of solar air heater.
3. Model with 5cm staggered arrangement NACA Airfoil fins is the design that provides the best overall performance for a solar air heater.

For future recommendation, more experiment based researches about solar air heater using airfoiled extended surface should be done, so that the results obtained from experiment can be compared with results from simulation and come up with a more convincing conclusion.

REFERENCE

[1] A. A. El-Sebaii, S. Aboul-Enein, M. R. I. Ramadan, S. M. Shalaby, and B. M. Moharram, "Thermal performance investigation of double pass-finned plate solar air heater," *Appiled Energy,* vol. 88, pp. 1727-1739, 18th December 2010 2011.

[2] A. Priyam and P. Chand, "Thermal and thermohydraulic performance of wavy finned absorber solar air heater," *Solar Energy,* vol. 130, pp. 250-259, 27th February 2016 2016.

[3] C.-D. Ho, H. Chang, R.-C. Wang, and C.-S. Lin, "Performance improvement of a double-pass solar air heater with fins and baffles under recycling operation," *Appiled Energy,* vol. 100, pp. 155-163, 7th May 2012 2012.

[4] F. Chabane, N. Moummi, and S. Benramache, "Experimental study of heat transfer and thermal performance with longitudinal fins of solar air heater," *Journal of Advanced Research,* vol. 5, pp. 183-192, 10th April 2013 2014.

[5] H.-M. Yeh, C.-D. Ho, and J.-Z. Hou, "Upward-type flat-plate solar air heaters attached with fins and operated by an internal recycling for improved performance," *Journal of the Taiwan Institute of Chemical Engineers,* vol. 43, pp. 235-240, 13th November 2011 2012.

[6] M. F. El-khawajah, L. B. y. Aldabbagh, and F. Egelioglu, "The effect of using transverse fins on a double pass flow solar air heater using wire mesh as an absorber," *Solar Energy,* vol. 85, pp. 1479-1487, 27th April 2011 2011.

[7] M. Nems and J. Kasperski, "Experimental investigation of concentrated solar air-heater with internal multiple-fin array," *Renewable Energy,* vol. 97, pp. 722-730, 20th June 2016 2016.

[8] J. Kasperski and M. Nems, "Investigation of thermo-hydraulic performance of concentrated solar air-heater with internal multiple-fin array," *Appiled Thermal Engineering,* vol. 58, pp. 411-419, 4th May 2013 2013.

[9] T. H. Kim, J. G. Kwon, S. H. Yoon, H. S. Park, M. H. Kim, and J. E. Cha,

"Numerical analysis of air-foil shaped fin performance in printedcircuit heat exchanger in a supercritical carbon dioxide power cycle," *Nuclear Engineering and Design*, vol. 288, pp. 110-118, 9th March 2015 2015.

[10] W. L. Siauw, J.-P. Bonnet, J. Tensi, L. Cordier, B. R. Noack, and L. Cattafesta, "Transient dynamics of the flow around a NACA 0015 airfoil using fluidic vortex generators," *International Journal of Heat and Fluid Flow,* vol. 31, pp. 450-459, 19th March 2010 2010.

[11] A. S. Yadav and J. L. Bhagoria, "Heat transfer and fluid flow analysis of solar air heater: A review of CFD approach," *Renewable and Sustainable Energy Review,* vol. 23, pp. 60-79, 21th March 2013 2013.

[12] A. Saxena, Varun, and A. A. El-Sebaii, "A thermodynamicreviewofsolarairheaters," *Renewable and Sustainable Energy Reviews,* vol. 43, pp. 863-890, 6th December 2014 2015.

[13] A. A. Hegazy, "Numerical analysis of air-foil shaped fin performance in printedcircuit heat exchanger in a supercritical carbon dioxide power cycle," *Renewable Energy,* vol. 18, pp. 283- 304, 5th November 1998 1999.

[14] A. A. Hegazy, "Performance of flat plate solar air heaters with optimum channel geometry for constant/variable flow operation," *Energy Conversion & Management,* vol. 41, pp. 401-417, 22th January 1999 2000.

[15] H.-M. Yeh, C.-D. Ho, and J.-Z. Hou, "The improvement of collector efficiency in solar air heaters by simultaneously air flow over and under the absorbing plate," *Energy* vol. 24, pp. 857-871, 25th October 1998 1999.

[16] O. Mahfoud, M. Zedayria, A.Moummi, and N. Moummi, "Numerical 2D study of air flow controlled by passive technique in solar air collectors," *Review of Renewable Energies,* vol. 16, pp. 159-170, 29th March 2013 2013.

[17] S. Vyas and D. S. Punjabi, "THERMAL PERFORMANCE TESTING OF A FLAT PLATE SOLAR AIR HEATER USING OPTICAL MEASUREMENT TECHNIQUE," *International Journal of Recent advances in Mechanical Engineering (IJMECH),* vol. 3, November 2014 2014.

[18] A. C. Yunus and J. G. Afshin, *Heat and Mass Transfer 5th Edition :*

Fundamentals and Applications, 2011.

[19] O.-S. Gim and G.-W. Lee, "Flow characteristics and tip vortex formation around a NACA 0018 foil with an endplate," *Ocean Engineering*, vol. 60, pp. 28-38, 26th January 2013 2013.